

THESIS FOR THE DEGREE OF LICENTIATE OF ENGINEERING

A toolbox for improving the processability of  
composites with a high content of thermomechanical pulp

Seyedehsan Hosseini



Department of Chemistry and Chemical Engineering

CHALMERS UNIVERSITY OF TECHNOLOGY

Gothenburg, Sweden 2021

# A toolbox for improving the processability of composites with a high content of thermomechanical pulp

Seyedehsan Hosseini

© Seyedehsan Hosseini, 2021.

Licentiatuppsatser vid Institutionen för kemi och kemiteknik

Chalmers tekniska högskola.

Nr 2021:17

Department of Chemistry and Chemical Engineering

Chalmers University of Technology

SE-412 96 Gothenburg

Sweden

Telephone: + 46 (0)31-772 1000

Cover: From fibers to composite, with a high content of thermomechanical pulp

Printed by Chalmers Reproservice

Gothenburg, Sweden 2021

# **A toolbox for improving the processability of composites with a high content of thermomechanical pulp**

Seyedehsan Hosseini  
Department of Chemistry and Chemical Engineering  
Chalmers University of Technology

## **ABSTRACT**

The use of oil-based products causes large volumes of non-biodegradable waste and contributes to climate changes. Focus has consequently shifted towards the use of polymers derived from wood. The processability of such polymers, however, presents a challenge but this can be overcome through the use of composite materials, i.e., a blend of wood-derived material and fossil fuel-based polymers. Wood-derived material requires either additives or modification in order to achieve high loading of the renewable polymer section. Two possible routes for modifying thermomechanical pulp (TMP) are outlined here, with the aim of achieving composites with a high content of TMP that not only have good mechanical properties but are also processable. The addition of physical modifiers, such as magnesium stearate (MgSt) and molybdenum disulfide ( $\text{MoS}_2$ ), and their effects on the matrix of polyolefin copolymer poly(ethylene-co-acrylic acid (EAA)) in the TMP loading were the first route studied. The composites were prepared by compression moulding and had dry TMP contents of 30, 50 and 70 wt%, respectively, and 5 wt% additive relative to the weight of TMP. The second route was chemical modification of TMP fibres using three different alkyl ketene dimers (AKD), and was tested within the matrix of polypropylene (PP). The AKDs had carbon chains that were 6, 12 and 18 carbons in length. The AKD-modified TMP was extruded with PP at 50 wt% TMP. The addition of TMP increased the mechanical strength of the composites, independent of matrix (EAA or PP). The addition of MgSt or  $\text{MoS}_2$  increased the strength of the TMP-EAA composites further. Also, the presence of  $\text{MoS}_2$  improved the interface compatibility between EAA and TMP, as revealed by the use of rheology. In the case of AKD-modified TMP, surface energy measurements showed that modification reduced the surface energy of the fibres and increased hydrophobicity. The colour, shape of the extruded filament and reduced complex viscosity all indicate the easier processability of the TMP modified with the longest AKD carbon chain. It may be concluded that both the physical and chemical modifications made showed improvements in the processability of these composites.

**Keywords:** thermomechanical pulp, magnesium stearate, molybdenum disulfide, AKD, composite, mechanical properties, interface.

## LIST OF PAPERS

- I. Seyedehsan Hosseini, Abhijit Venkatesh, Antal Boldizar and Gunnar Westman. Molybdenum disulphide - A traditional external lubricant that shows interesting interface properties in pulp-based composites. *Journal of Polymer composites*, 2021, Volume 42, Issue 7, Pages 4884-4896.
- II. Seyedehsan Hosseini, Robin Nilsson, Anette Larsson, Anna Ström and Gunnar Westman. Alkyl ketene dimer modification of thermomechanical pulp promotes compatibility with polypropylene. Manuscript.

## **CONTRIBUTION REPORT**

- I. Planning the experiments with the co-authors; conducting all the experiments; performing the chemical, thermal and mechanical analyses; and writing the manuscript with the support of the co-authors.
- II. Planning the experiments; conducting all the experiments including their synthesis and processing; performing the chemical, thermal and mechanical analyses; and writing the manuscript with the support of the co-authors.

## ABBREVIATIONS

AKD	Alkyl ketene dimer
ATR-FTIR	Attenuated total reflectance- Fourier transform infrared spectroscopy
$B_{\text{swell}}$	Die ratio
DMA	Dynamic mechanical analysis
EAA	Ethylene-co-acrylic acid
EDX	Energy-dispersive X-ray spectroscopy
MgSt	Magnesium stearate (Mg (st) <sub>2</sub> )
NMR	Nuclear magnetic resonance spectroscopy
PE	Polyethylene
PP	Polypropylene
PS	Polystyrene
PVC	Polyvinyl chloride
RBF	Round bottom flask
SEM	Scanning electron microscopy
TMP	Thermomechanical pulp
WPC	Wood-polymer composite

# 1 Table of Contents

1	Table of Contents .....	7
1.	Introduction.....	9
1.1	Aim .....	10
2	Background.....	11
2.1	Thermomechanical pulp (TMP).....	11
2.1.1	Cellulose .....	11
2.1.2	Lignin.....	12
2.1.3	Hemicellulose.....	12
2.2	Wood-based composites .....	12
2.2.1	Polymers for pulp fibre composites .....	12
2.3	TMP-polymer interface and the effects of modification.....	13
3	Materials & Methods .....	16
3.1	Materials .....	16
3.2	Methodology.....	16
3.2.1	TMP – EAA composites .....	16
3.2.2	Synthesizing AKD from fatty acyl chlorides.....	16
3.2.3	Chemical modification of TMP fibres .....	17
3.2.4	Production of paper sheets .....	18
3.2.5	Compounding modified and unmodified TMP fibres with PP .....	18
3.2.6	Attenuated total reflectance-Fourier transform infrared spectroscopy (ATR-FTIR)....	19
3.2.7	Scanning electron microscopy (SEM) and energy-dispersive X-ray spectroscopy (EDX) .....	19
3.2.8	Nuclear magnetic resonance spectroscopy (NMR).....	19
3.2.9	Contact angle and surface energy .....	19
3.2.10	Tensile testing .....	20
3.2.11	Dynamic mechanical analysis (DMA) .....	20
3.2.12	Notched Izod impact strength test.....	21
3.2.13	Rheology .....	21
4	Results and Discussion .....	22
4.1	Adsorption of MgSt, MoS <sub>2</sub> and AKD molecules on the TMP fibres.....	22
4.2	Hydrophobization and surface energy of chemically-modified TMP fibres.....	23
4.3	The influence of MgSt, MoS <sub>2</sub> and AKD modification on the surface structure of TMP fibres .....	25
4.4	The effects of MgSt, MoS <sub>2</sub> and AKD on the mechanical properties of TMP composites....	27
4.5	The effects of MgSt and MoS <sub>2</sub> on the interfacial properties of the composites.....	29

4.6	Melt shear viscosity and visual impression of modified and unmodified TMP-PP composites .....	32
5	Conclusions.....	37
6	Future work.....	37
7	Acknowledgments.....	38
8	Bibliography .....	39
9	Appendix.....	47
9.1	NMR spectra of synthesized AKD.....	47
9.2	Water drop volume and water contact angle over time.....	48
9.3	Thermal degradation of the modified TMP fibres .....	49



## 1. Introduction

Environmental issues have entailed efforts being made nowadays to reduce the usage of plastics and synthetic polymers in industry as well as in everyday life<sup>1,2</sup>. The main challenge being faced is replacing these plastics and synthetic polymers with a more natural-based material. Such a raw material must be able to compete with the existing, widely-used plastics with respect to price, processability and mechanical properties of the final material.

Despite comprising less than one percent of the planet's forested land, Sweden is the world's second biggest exporter of pulp, paper and sawn timber products. The total land area of Sweden covers 40.8 million hectares, 22.5 million of which are productive forest land. The growth of the forests is greater than the amount felled, and has been so for the entire 20th century onwards<sup>3</sup>; the use of natural fibres from trees can therefore be one of the potential options that are open. Sawdust and thermomechanical pulp (TMP) fibres are one of the cheapest materials currently available from the forest, and both can be competitive in price relative to existing plastics. Indeed, wood-polymer composites (WPCs) have been commercial products since the 1960's: they are nevertheless mostly reinforced with sawdust or wood powder to a maximum of 70 wt%<sup>4</sup>, both of which behave as fillers and thus lack the reinforcement ability of fibres<sup>5</sup>. TMP fibres, on the other hand, have been shown to improve the mechanical properties of wood-polymer composites<sup>6</sup>. However, in the case of fibre-reinforced composites, WPCs containing a wide range of TMP fibres (30 wt% or lower<sup>6</sup>, 50 wt%<sup>7,8</sup> and 60 wt%<sup>9</sup>) has already been studied; in almost in all of the studies, the greatest problem was fibre entanglement encountered during processing.

It has been widely confirmed that a key component to attaining good composite properties relies on the interface and the compatibility of the matrix with the filler. In the wood fibre-polyolefin system, mixing the relatively polar lignocellulosic surface of TMP with a non-polar polymer is the main challenge. Moreover, wood fibres have a tendency to self-aggregate during the melt processing<sup>10-15</sup>. Two main methods were used to overcome the poor interface between TMP and the matrix, and to increase the processability of high content TMP-based composites, namely physical modification (i.e. the addition of additives and lubricants) and chemical modification.

Molybdenum disulfide (MoS<sub>2</sub>) has the ability to interact with the aromatic structure in lignin<sup>16,17</sup> and was chosen as the external lubricant in this study, whilst magnesium stearate

(MgSt)<sup>18-20</sup>, which is currently used as a sizing agent in the papermaking process because it improves the flow properties of the mixture during the melting processing by reducing viscosity, was chosen as the internal lubricant.

The use of sizing agents is one of the most popular methods employed in the pulp and paper industry for altering the hydrophilic nature of lignocellulosic surfaces: alkyl ketene dimers (AKD) in particular are commonly used<sup>21,22</sup>. The most important feature of an AKD is the dual polarity of its structure: a polar component to react with the cellulose surface and a nonpolar (hydrophobic) component that should be compatible with polyolefins<sup>15</sup>. Some studies, such as the work of Quillin *et al.*, have investigated the effects of AKD modification on bleached kraft cellulose pulp to form a composite with polypropylene (PP)<sup>15</sup>.

In the first study EAA copolymer, which is an aqueous polymer dispersion with minimal or even no presence of other solvents or emulsifiers<sup>23,24</sup>, was used as a matrix for the TMP-based biocomposites. MoS<sub>2</sub> and MgSt were used as lubricants and additives with the aim of overcoming the aforementioned issues on loading. In the second study, PP was used as the matrix and AKD modification of the TMP fibres was employed to overcome the above challenges faced in an extrusion process.

## 1.1 Aim

The aim of this work was to improve the interface between TMP fibres and polyolefin matrices. Two methods were employed to this end: in the first study, the surface of TMP fibres was modified using the additives MgSt and MoS<sub>2</sub>. MgSt is widely used in pharmaceutical industries and has shown potential in applications for modifying cellulose, whereas it is hypothesized that MoS<sub>2</sub> interacts with TMP via lignin and thereby improves the interface between the matrix and the TMP fibres. In the second study, chemical modification was used to modify the surface of the TMP fibres to increase their hydrophobicity and thus increase compatibility between the fibres and the matrix.

## 2 Background

### 2.1 Thermomechanical pulp (TMP)

TMP is produced by processing wood chips using heat and mechanical refining. Mechanical refining is an established technology in the pulp and paper industry: its purpose is to separate fibre bundles and to create a high surface area by fibrillation of the cell wall structures<sup>25</sup>. TMP consists of approx. 40% cellulose, 30% hemicellulose and 30% lignin<sup>26</sup>.

A TMP fibre has several different layers. Notably rougher than the inner layers, the outer fibre walls are comprised mainly of lignin, hemicelluloses and a small amount of cellulose microfibrils that together form an irregular network structure. The inner layers, on the other hand, generally consist of cellulose. The majority of the cellulose is located in the secondary cell wall layers, which have a homogeneous fibrillar structure<sup>27,28</sup>.

#### 2.1.1 Cellulose

Cellulose is the essential component of all plant fibres. The organization of cellulose chains is achieved by both hydrogen bonds and hydrophobic interactions<sup>29</sup>. Four major types of cellulose allomorphs have been reported (Cellulose I, II, III and IV) on the basis of their X-ray diffraction patterns<sup>29</sup>. The natural form of cellulose, known as Cellulose I, is the most important crystalline form of cellulose and is the most abundant type: it can occur as  $\alpha$  and  $\beta$  allomorphs. Cellulose I $\beta$  is close to the model proposed in the literature, while the crystalline structure of Cellulose I $\alpha$  is still being discussed<sup>29</sup>. Solid cellulose forms a microcrystalline structure with regions of high order (i.e. crystalline regions) and regions of low order (i.e. amorphous regions)<sup>30</sup>. The various structural levels of a plant cell wall are shown schematically in Figure 1.

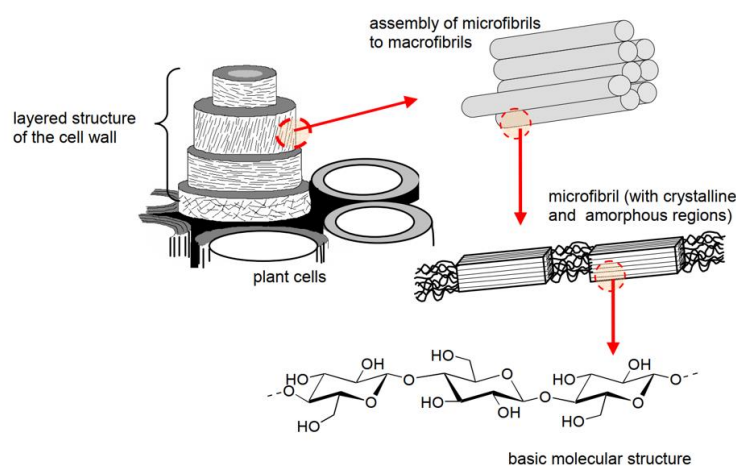


**Figure 1.** Schematic diagram of the different structural levels of cellulose. (reproduced from PhD thesis of Hassani, M.<sup>26</sup>)

### 2.1.2 Lignin

Lignin is the second most abundant biopolymer in the world after cellulose; situated on the surface of the fibre<sup>26</sup>, it has a concentration in wood ranging from 20% to 30%<sup>31</sup>. A complex hydrocarbon polymer, lignin has both aliphatic and aromatic structures: it is the key structural material in the support tissues of vascular plants and some algae. Lignin is the adhesive, or binder, in wood that holds the fibres together and it is highly concentrated in the middle lamella plant cells. It has a glass transition temperature ( $T_g$ ) of approx. 130-150°C<sup>32</sup>, and its mechanical strength is less than that of cellulose<sup>6,26</sup>.

### 2.1.3 Hemicellulose

Hemicelluloses are a group of polysaccharides (excluding pectin) that remain associated with the cellulose after lignin has been removed: despite the nomenclature, they are not a form of cellulose. From a chemical perspective, hemicelluloses are a class of polymers of sugars that includes the six-carbon sugars mannose, galactose, glucose and 4-O-methyl-D-glucuronic acid and the five-carbon sugars xylose and arabinose<sup>32</sup>. From a physical perspective, hemicelluloses are rarely crystalline or fibrous in nature. It is interesting to note that the presence of hemicelluloses on cellulose fibres increases the strength of paper<sup>30</sup>.

## 2.2 Wood-based composites

### 2.2.1 Polymers for pulp fibre composites

Polymers can be categorized as being either thermoplastics or thermosets. Thermoplastic polymers are amorphous or semi-crystalline which, as the temperature increases, soften continuously. Polyethylene (PE), polystyrene (PS), polyvinyl chloride (PVC) and PP are all examples of synthetic thermoplastics. Thermosets, on the other hand, polymerize and stiffen as the temperature increases: their molecular chains are regular in order, with strong intermolecular bonds. Vinyl esters, phenol formaldehyde, polyester and epoxy resin<sup>33,34</sup> are examples of thermosets. Compared to thermosets, thermoplastics are economically favourable, have a faster processing route and are recyclable, and are therefore used more often nowadays in wood fibre composites<sup>30</sup>. The processing conditions dictate that the thermoplastic polymers used in wood-based composites have a lower softening temperature than the thermal degradation of the wood components, e.g. polyolefins such as PP (see Figure 2a)<sup>30,35,36</sup>. The nature of the interface between the polymer and the pulp is highly important because it influences how the properties of the fibre are transformed into the biocomposite, and vice versa. The nature of the interface of different polymer matrices should therefore be explored in an

attempt to develop guidelines for the selection of materials that would optimize mechanical properties and promote processability<sup>33</sup>.

EAA copolymer is another favourable thermoplastic candidate for use in natural fibre composites because its low processing temperature reduces the risk of thermal degradation of the cellulose fibres<sup>37</sup>. In addition, EAA has the carboxylic functional groups on its surface: these groups make it more hydrophilic compared to PP, see Figure 2b, so it may be more compatible with TMP than other thermoplastics.

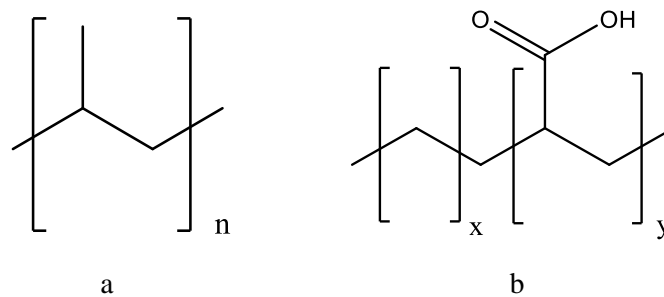


**Figure 2.** Structures of (a) PP and (b) EAA copolymer.

### 2.3 TMP-polymer interface and the effects of modification

The interface between the matrix and the filler is a key component to good composite properties, as mentioned previously. In many cases, inferior mechanical properties and the low processability of a wood fibre composite can be attributed to the weak fibre–matrix interfacial bond caused by low compatibility<sup>38</sup>. Poor connections between the fibres and the matrix promote large-scale debonding (separation of the fibre-matrix in the composite interface), thereby reducing the load transfer between fibre-matrix<sup>39</sup>. Obviously, an important key to the successful processing of wood fibre composite is finding a way of improving compatibility between matrix and fibres<sup>38</sup>, to which end both matrix resin modification and fibre surface treatment have been considered<sup>40,41</sup>. Maldas *et al.* have shown that the pretreatment of wood fibres to alter the chemical nature of the fibre surface is more promising than matrix resin modification<sup>12</sup>. As a rule, in interfacial coupling, the hydrophilic group of the coupling agent is expected to react chemically with the functional groups on the wood fibre surface and the hydrophobic group should react, or have relatively high compatibility with, the polymer matrix. The combined effects of these interactions will effectively improve the compatibility of the fibres and matrix<sup>38</sup>.

The main components of TMP, i.e. cellulose, hemicellulose and lignin, have a large number of polar hydroxyl groups and phenolic hydroxyl functional groups: these make the surface exhibit chemical polarity, and results in a poor fibre-matrix interface<sup>42</sup>.

Two main methods for improving the interface of the TMP fibres-matrix may be found in the literature: physical modification (using additives and lubricants) and chemical modification. Lubricants are divided into internal and external lubricants. Internal lubricants usually contain polar groups, such as carboxylic and amine groups, that interact with the alcohol groups of the fibre, whereas external lubricants usually lack polar chemical groups and normally reduce friction between the composite and metal surfaces or between the fibres and the matrix<sup>43</sup>.

Sangyeob Lee *et al.*<sup>44</sup> considered the effects of physical compatibilizers and additives, such as phenol formaldehyde and urea formaldehyde, on the interfacial properties of TMP fibres and PP. They came to the conclusion that these additives improved not only compatibility between the TMP fibres and PP, but also the tensile strength properties.

MoS<sub>2</sub> is an inorganic compound, which has shown good tribological behaviour when used as an external additive for lubrication in metal industries. Tribological tests confirm that the use of MoS<sub>2</sub> leads to significant reduction in both friction and wear under severe test conditions in boundary as well as mixed lubrication regimes. MoS<sub>2</sub>, which has also been shown to interact with the aromatic structure in lignin<sup>16,17</sup>, is the external lubricant chosen for use in this study.

One of the additives that has been used for cellulose is MgSt, which has also been used in the pharmaceutical and food industries. Although MgSt is a hydrophobic lubricant with the ability to increase the fluidity of microcrystalline cellulose (MCC), it could nevertheless cause an appreciable loss in strength since MCC compacts at lubricant concentrations exceeding 0.5%<sup>46,47</sup>.

Chemical modification of fibres has been ongoing since the 19th century, the most common types being etherification, esterification and oxidation, along with corresponding crosslinking reactions based on the polyfunctionality of cellulose<sup>26,48</sup>.

Rozman *et al.*<sup>49</sup> investigated the modification of TMP with silane and its effects on the properties of a TMP-urea formaldehyde composite in a compression moulding process. They concluded that, when compared to the unmodified TMP, the silane system works like a wax, improving the elasticity of the composites. Maleated PP is one of the polymers that can be used instead of PP, as there is some evidence of its reaction with cellulose<sup>48</sup>. The interaction between

TMP and maleated PP has been investigated, and no evidence of any reaction between TMP and maleated PP has been presented thus far: it seems instead that the lignin in the TMP fibres hinders the reaction<sup>50-52</sup>.

Maleic anhydride and benzoyl peroxide are two other chemical coupling agents that have been employed to improve the interfacial properties of TMP fibre and PP. In one study, where a mix of these two chemical couplings was used to improve the interfacial properties, SEM images showed that fibre pullouts in the mechanical failure were less than those of unmodified fibres in the composites<sup>53</sup>. Fewer fibre pullouts are an indication of an improved interphase between PP and the TMP fibres. A similar study of the interfacial properties of benzoylated and lauroylated TMP fibres-PP using mechanical analysis and SEM images found that the compatibility between TMP fibres-PP improved<sup>54</sup>. Studying AKD modification as the lauroylated TMP is therefore motivated, as TMP-modified AKD has a similar structure.

Esterification is a common method for modifying the surface of TMP in order to reduce surface hydrophilicity and improve thermal properties, thereby allowing for the preparation of composites in the future<sup>55</sup>. AKD, which is one of the most important components for modifying pulp fibres chemically, is used widely in the pulp and paper industry for the hydrophobization of fibre surfaces<sup>56</sup>. It is generally believed that AKD reacts with the cellulose present in the fibres to form a beta-keto ester bond, which substitutes the OH groups and makes the fibres more hydrophobic<sup>57</sup>. In the chemical modification study, the AKD reaction was used as the main method for modifying the TMP fibres chemically. A schematic diagram of the reaction between AKD and cellulose is shown in Figure 3.

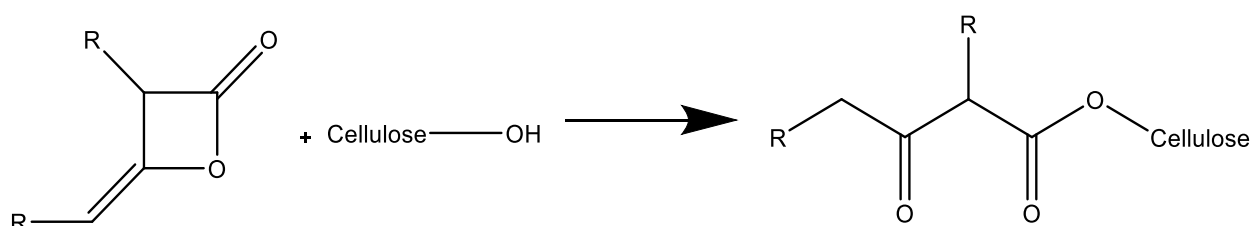


**Figure 3.** Schematic diagram of the AKD and cellulose reaction.

## 3 Materials & Methods

### 3.1 Materials

The TMP used was made from *Picea abies* (Norway spruce) and kindly provided by StoraEnso Hyltebruk, Sweden. Fibre analysis of the TMP, performed using a Kajaani FS300 fiber analyser, gave a mean fibre length, width and fines distribution of 3.2 mm, 35  $\mu\text{m}$  and 3 %, respectively<sup>58</sup>. BIM Kemi AB, Sweden, supplied the EAA copolymer, further information of which can be found in Paper I<sup>58</sup>. MoS<sub>2</sub> and MgSt were both obtained from Sigma Aldrich, Germany. According to the supplier, the MoS<sub>2</sub> was not exfoliated, had a density of 5.06 g/ml and a particle size of less than 2  $\mu\text{m}$ ; the MgSt had a density of 1.026 g/cm<sup>3</sup> and a melting point of 200 °C. The fatty acyl chlorides were purchased from Sigma Aldrich, Germany, who stated that the PP had a melt flow rate (MFR) of 100 g/min, a density of 0.902 g/mL and a melting point of 160°C.

The butyl acetate, diethyl ether, ethylene glycol, polyethylene glycol and formamide used were all purchased from Sigma Aldrich, Germany.

### 3.2 Methodology

#### 3.2.1 TMP – EAA composites

The TMP fibres, EAA dispersion and an additive (MgSt or MoS<sub>2</sub>) were mixed at different proportions to obtain the desired pulp weight fractions of dried composites given in Table 1. Compression moulding was the method chosen for the first study, see Paper I for detailed information of the process conditions<sup>58</sup>.

#### 3.2.2 Synthesizing AKD from fatty acyl chlorides

Triethylamine was dissolved in butyl acetate in a round-bottomed flask (RBF). A stoichiometric amount of fatty acid chloride (stearoyl chloride, lauryl chloride or hexanoyl chloride) was dissolved in butyl acetate in a beaker, and then added dropwise to the RBF while stirring. After adding the whole amount of fatty acid chloride, the reaction temperature was set at 45 °C for 2 hours. At the end of the reaction, the AKD was filtered from the salt using diethyl ether, and the residual solution evaporated in a rotary evaporator. The AKDs derived from hexanoyl chloride, lauryl chloride and stearoyl chloride are referred to hereafter as AKD Hex, AKD Lau and AKD St, respectively.



**Table 1.** The samples with their designated compositions of TMP, additive and EAA.

Sample designation	Pulp (wt%)	Additive (wt%)	EAA (wt%)
TMP	100	0	0
EAA	0	0	100
EAA-MoS <sub>2</sub>	0	0.5	99.5
		1.5	98.5
		5	95
TMP30	30	0	70
TMP50	50	0	50
TMP70	70	0	30
TMP30-MgSt, TMP30-5MgSt	30	1.5	68.5
		5	65
TMP50-MgSt,	50	2.5	47.5
TMP70-MgSt,	70	3.5	26.5
TMP30-MoS <sub>2</sub> ,	30	1.5	68.5
TMP30-5MoS <sub>2</sub>		5	65
TMP50-MoS <sub>2</sub>	50	2.5	47.5
TMP70-MoS <sub>2</sub>	70	3.5	26.5
EAA-TMP30- MgS+MoS <sub>2</sub> EAA-TMP30- 5(MgSt+MoS <sub>2</sub> )	30	0.75+0.75	68.5
		2.5+2.5	65
EAA-TMP50- MgSt+MoS <sub>2</sub>	50	1.25+1.25	47.5

### 3.2.3 Chemical modification of TMP fibres

The TMP fibres were soaked in deionized water for 30 minutes before being filtered and spread out on a sheet of aluminium foil. The different AKD molecules were dissolved in ethanol and then sprayed onto the TMP fibres: the AKD:TMP molar ratio was approx. 20:100. The systems were subsequently placed in an oven for 2 hours at 90 °C, after which the fibres were washed

in 40 °C ethanol in a RBF to remove all of the weakly attached AKD. Finally, the fibres were filtered and washed twice with deionized water and ethanol at ambient temperature. The fibres were placed in a fume hood for 1 day prior to use.

### 3.2.4 Production of paper sheets

An amount of mass suspension corresponding to 2 sheets (unmodified and modified TMP) was measured and diluted in 1L of deionized water before being mixed at room temperature in a L&W pulp disintegrator (Lorentzen & Wettre) for 60,000 revolutions at 2900 rpm. Thereafter the sheets were made according to the TAPPI T 205 method. They were air dried for one week and placed under a 10-ton press for one day to obtain a smooth surface area. A sheet with a surface weight of 60 g/m<sup>2</sup> weighed 1.285 g.

### 3.2.5 Compounding modified and unmodified TMP fibres with PP

Two batches of TMP (AKD-modified or unmodified) and PP were used to produce PP-TMP composites (a total of 12 g of composite for each sample). The materials were compounded for 10 min at 120 °C and then extruded using a Haake Minilab 3 Micro Compounder, which is a conical twin-screw compounder with an integrated backflow channel. The extruded material was melted at 190 °C in a hot press, at a pressure of 5 tons for 5 min, followed by a pressure of 10 tons for another 5 min. The material was then cooled to room temperature, resulting in plates of 0.5 mm in thickness. The pressed material was cut into test bars (known as “dog bones”) with a width, thickness and length of 4, 1 and 40 mm, respectively.

**Table 2.** The samples with their designated weight percentages of TMP fibre, AKD and PP.

Sample designation	TMP (wt%)	AKD (wt%)	PP (wt%)	AKD/TMP (wt%)	AKD/TMP (mol%)
PP	0	0	100	---	---
PP-TMP	50	0	50	0	0
PP-TMP AKD Hex	50	10	40	20	12
PP-TMP AKD Lau	50	12.5	37.5	25	20
PP-TMP AKD St	50	15	35	30	20

### 3.2.6 Attenuated total reflectance-Fourier transform infrared spectroscopy (ATR-FTIR)

ATR-FTIR was performed using a Perkin Elmer Frontier FT-IR Spectrometer (Waltham, MA, USA) equipped with a diamond GladiATR attenuated total reflectance (ATR) attachment from Pike Technologies. The samples, which were measured in triplicates, were placed directly on the ATR-crystal without further preparation. The spectra were recorded between 4000 and 400  $\text{cm}^{-1}$ , with 20 scans being collected with a resolution of 4  $\text{cm}^{-1}$  at intervals of 0.5  $\text{cm}^{-1}$ .

### 3.2.7 Scanning electron microscopy (SEM) and energy-dispersive X-ray spectroscopy (EDX)

The surface morphology of pulp fibres was imaged using a field emission scanning electron microscope (SEM - FEI Quanta 200 FEG ESEM), employing a low acceleration voltage (10 kV). The samples were not conductive, so each one was attached to a strip of carbon tape before a low pressure of 0.2-1 bar was applied to the chamber. EDX analysis was performed using the same machine and set-up.

### 3.2.8 Nuclear magnetic resonance spectroscopy (NMR)

Solution phase NMR was used to verify synthesized AKD molecules. The spectra were recorded at room temperature on a Varian MR-400 (Varian, Palo Alto, CA, USA) operating at 399.95 MHz for proton detection and 100.58 MHz for carbon detection. Chloroform-d was used as the solvent for all samples.

### 3.2.9 Contact angle and surface energy

Using Equation 1, and measuring the contact angle of different liquids of which the surface tension components are known on the same solid surface, the surface energy can be measured<sup>59</sup> thus:

$$\frac{1+\cos\theta}{2} \times \frac{\sigma_l}{\sqrt{\sigma_l^d}} = \sqrt{\sigma_s^p} \times \sqrt{\frac{\sigma_l^p}{\sigma_l^d}} + \sqrt{\sigma_s^d} \quad \text{Eq 1.}$$

where,  $\sigma_s = \sigma_s^p + \sigma_s^d$  is the solid surface free energy,  $\sigma_l$  is the liquid surface tension, d and p are the dispersive and polar components of the liquid surface tension and solid surface energy, respectively, and  $\theta$  is the contact angle formed between the liquid drop and the solid surface.

This allows  $\frac{1+\cos\theta}{2} \times \frac{\sigma_l}{\sqrt{\sigma_l^d}}$  versus  $\sqrt{\frac{\sigma_l^p}{\sigma_l^d}}$  to be plotted. The points can then be fitted to a straight line in order to calculate  $\sigma_s^p$  and  $\sigma_s^d$ , respectively, from the slope and from the intersection with

the vertical axis, before deriving the total solid surface free energy that is the sum of  $\sigma_s^p$  and  $\sigma_s^d$ .<sup>59</sup>

The contact angles of the liquids and substrates were determined using a theta optical tensiometer (Attension, Finland); the same method was used in this work as the TAPPI standards employed by Moutinho *et al.*<sup>59</sup>. The initial resting drop image (<3 s after application of the liquid) was acquired by a charge-coupled device camera. Five liquids were used as probes; the data values of the total surface tension and the corresponding dispersive and polar components as measured by Moutinho *et al.*<sup>59</sup> are presented in Table 3.

**Table 3.** The surface tension, polar and dispersive components of the solvents used, as determined by Moutinho *et al.*<sup>59</sup>.

Liquid	Surface tension, $\sigma_1$ (mN/m)	Polar component, $\sigma_1^p$ (mN/m)	Dispersive component, $\sigma_1^d$ (mN/m)
Deionized water	72.8	48.1	24.7
Deionized water /Ethylene glycol	57.7	39.1	28.5
Formamide	58.1	25.8	32.3
Ethylene glycol	48.3	17.4	30.9
Propylene glycol	35.4	9	26.4

### 3.2.10 Tensile testing

Tensile test bars, with a gauge length of 20 mm, were cut from the compression moulded specimen. The tensile properties (Young's modulus, stress at break and elongation at break) were measured at room temperature with a strain rate of 6 mm/min using a Zwick/ Z2.5 tensile tester, a grip-to-grip separation of 40 mm and a load cell of 2 kN.

### 3.2.11 Dynamic mechanical analysis (DMA)

The dynamic-mechanical properties were measured using a Rheometrics RSA II at room temperature (25 °C) at a frequency of 1 Hz. The samples were pre-strained in tension by about

0.15% which was kept constant during the measurements and subjected to a sinusoidal deformation with a strain amplitude which was increased from about 0.009% to 0.14%.

### 3.2.12 Notched Izod impact strength test

The impact strength of notched Izod specimens was measured according to ISO 180 in a Tinius Olsen testing machines: a Model 92T plastics impact tester with a 0.936 kg pendulum.

### 3.2.13 Rheology

Oscillatory shear rheology measurements were made with a DHR-3 (TA Instruments) using a parallel plate geometry (diameter = 25 mm, gap = 4000  $\mu\text{m}$ ) at 180 °C. The temperature was controlled using an environmental test chamber (ETC) provided by TA Instruments. Measurements were performed at a strain of 0.25 % between frequencies of 0.1 and 100 Hz.

## 4 Results and Discussion

### 4.1 Adsorption of MgSt, MoS<sub>2</sub> and AKD molecules on the TMP fibres

The adsorption of MgSt and MoS<sub>2</sub> onto TMP fibres was investigated based on the EDX analyses carried out on the samples. Figure 4 shows the elemental mapping of C, O, Mg, S and Mo of each respective sample. In the case of TMP fibres containing MgSt (Figure 4a), Mg was detected at the position that exhibited a higher intensity of carbon. This suggests that both Mg and carbon-rich molecules, such as alkanes, are present and thereby indicates the adsorption of MgSt onto the TMP samples. Figure 4b shows elements of 95 wt% TMP + 5 wt% MoS<sub>2</sub>, indicating that the contents of Mo and S match and thus confirming the presence of MoS<sub>2</sub> in the samples.

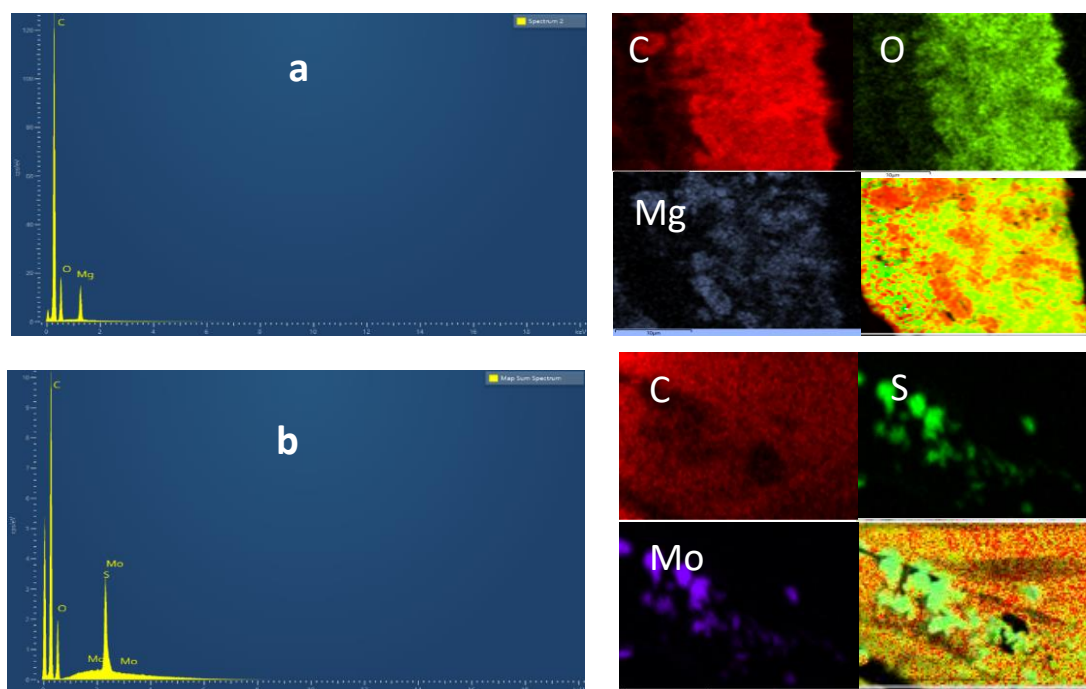


**Figure 4.** EDX analyses of 95 wt% TMP with (a) 5 wt% MgSt and (b) 5 wt.% MoS<sub>2</sub>, elemental mapping of C,O, Mg , S and Mo, and the combination of the components.

In the case of the reaction of AKD with TMP fibres, an esterification reaction is supposed to occur: the OH groups on the cellulose are substituted by an ester group connected to an alkyl chain. Figure 5 shows the IR spectra of TMP and TMP-modified with AKD Hex, AKD Lau and stearoyl chloride AKD St. As can be seen in the figure, the intensity of the carbon chain peak at 2800-3000<sup>-1</sup> increased for both AKD Lau and AKD St. The carbon chain peak shows a smaller increase for TMP modified with AKD Hex compared to the others, and is probably related to its shorter carbon chain (C6). In addition, a new carbonyl peak is seen to emerge

between 1700-1750  $\text{cm}^{-1}$ , which is a confirmation of the carbonyl bond expected on the modified TMP. The carbonyl peak of both AKD Lau and AKD St is sharp and the frequency is lower, indicating that both attach on the TMP surface and can form both hydrogen and ester bonds<sup>60</sup>.

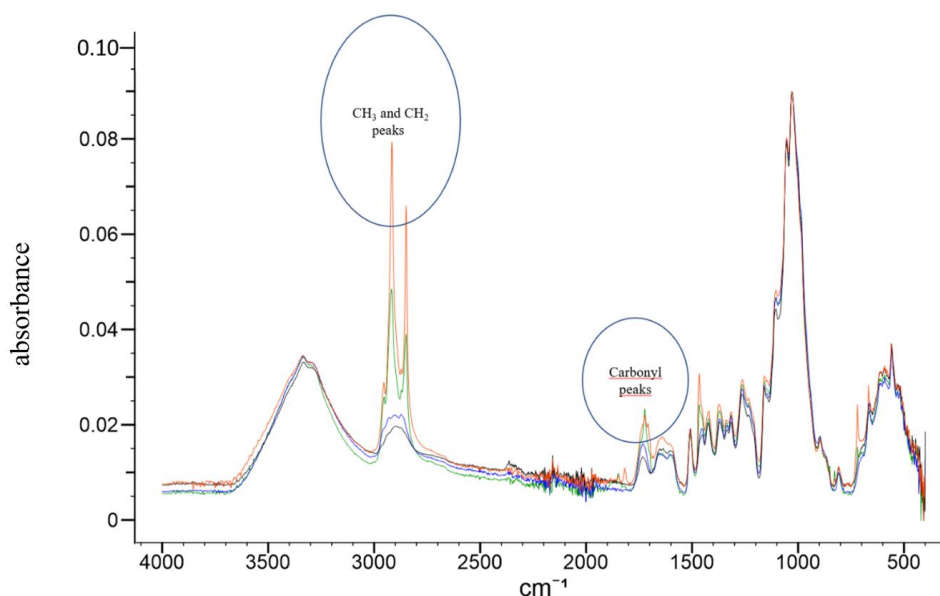


**Figure 5.** IR spectra of TMP (black), TMP modified with AKD from hexanoyl chloride (blue), lauryl chloride (green) and stearoyl chloride (red).

#### 4.2 Hydrophobization and surface energy of chemically-modified TMP fibres

The contact angles of different solvents on TMP and AKD-modified TMP are reported in Table 4. The contact angle increases for all liquids as the carbon chain length of the AKD increases, i.e. AKD Hex < AKD Lau < AKD St. Modifying TMP with a longer carbon chain AKD therefore increases the hydrophobicity of the surface.

**Table 4.** Contact angle ( $^{\circ}$ ) obtained for TMP and AKD-modified TMP for different liquids. The value of the contact angle is the average of at least 10 measurements, SD in parenthesis.

	Deionized water ( $^{\circ}$ )	Deionized water /ethylene glycol ( $^{\circ}$ )	Formamide ( $^{\circ}$ )	Ethylene glycol ( $^{\circ}$ )	Propylene glycol ( $^{\circ}$ )
TMP	82 (2)	68 (5)	54 (4)	41 (1)	47 (10)
TMP AKD Hex	95 (1)	105 (6)	68 (3)	90 (6)	60 (3)
TMP AKD Lau	110 (5)	107 (2)	107 (1)	99 (7)	67 (5)
TMP AKD St	120 (3)	108 (3)	112 (4)	104 (2)	100 (9)

Table 5 summarizes the results calculated for the different specimens in terms of the total polar and dispersive components and total surface free energy. The wettability of modified and unmodified TMP fibres was investigated by following the changes in volume of a water drop and the water contact angle as it progressed with time (see Appendix, Figures S2 and S3). In the case of unmodified TMP, both the volume of the water drop and its contact angle decreased with time until the drop was absorbed by the surface.

**Table 5.** Surface tension and the corresponding polar and dispersive components.

Sample	Polar component (mN/m)	Dispersive component (mN/m)	Total surface energy (mN/m)
TMP	4.8	28.9	33.7
TMP AKD Hex	0.2	26	26.2
TMP AKD Lau	0.1	15.2	15.3
TMP AKD St	0.8	6	6.8

All three AKD treatments reduced the polar and the dispersive component: the total surface energy of the TMP was thus in agreement with the studies of Carvalho *et al.*<sup>61</sup> and Huang *et al.*<sup>54</sup>. It is worth mentioning here that Graziano *et al.* have reported values of 0.4, 19.8 and 20.2 mN/m for the polar component, dispersive component and surface energy of PP, respectively, at 190 °C<sup>63</sup>. As can be seen in Table 5, all of the modifications decrease the polar component of the TMP fibre surfaces, which is regarded as being important for mixing PP with modified TMP fibres.



### 4.3 The influence of MgSt, MoS<sub>2</sub> and AKD modification on the surface structure of TMP fibres

SEM micrographs were taken in order to analyse the effects of the additives and AKD on the pulp fibres. In Figure 6 it can be observed that, unlike the unmodified TMP fibres, the modified ones have a coverage layer of lubricants.

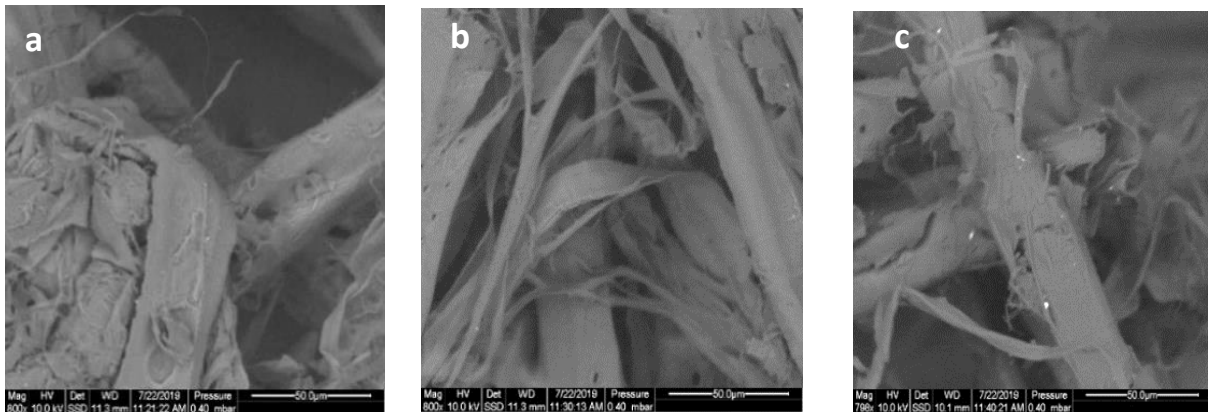


**Figure 6.** SEM images of (a) unmodified TMP fibres, (b) 95 % TMP + 5 % MgSt and (c) 95 % TMP+ 5 % MoS<sub>2</sub>. Magnification: 800x.

Figure 7 shows how the different AKD modifications influence the surface structure of the TMP fibres. No differences are visible in the SEM images of PP-TMP, PP-TMP AKD Hex and PP-TMP AKD Lau (Figure 7b, c & d), whilst those of PP-TMP AKD St (Figure 7e) show that the AKD St particles formed numerous flat platelets. Arminger *et al.*<sup>64</sup> investigated the effect of AKD wax (a mix of long chain AKDs) on the surface of beech wood powder and observed the same result, i.e. that long chain AKDs lead to numerous flat platelets forming on the surface of the fibres. They showed that AKD wax cause platelets to develop at certain temperatures (prior to the melting point being reached) and have a crystalline structure. In addition, a study carried out by Onda *et al.*<sup>65</sup> of AKD wax structures on superhydrophobic paper surfaces demonstrated a similar geometry.

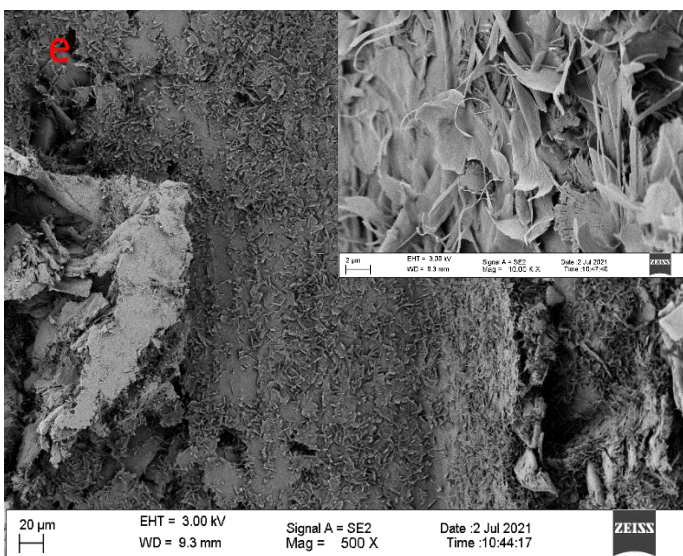
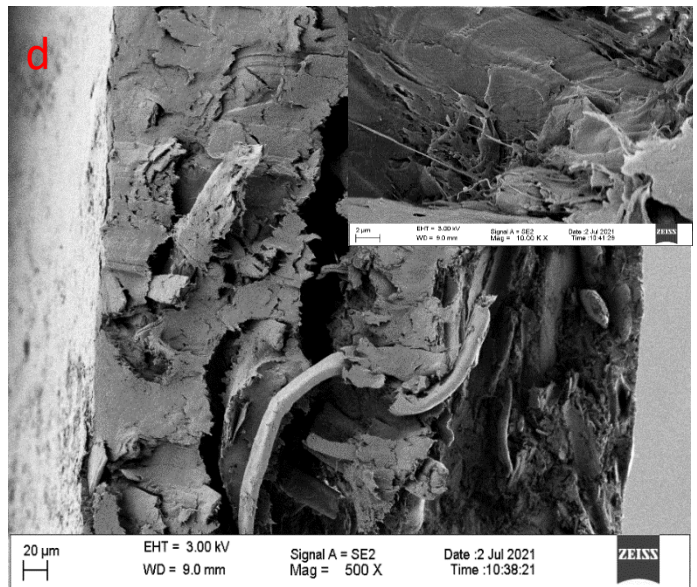
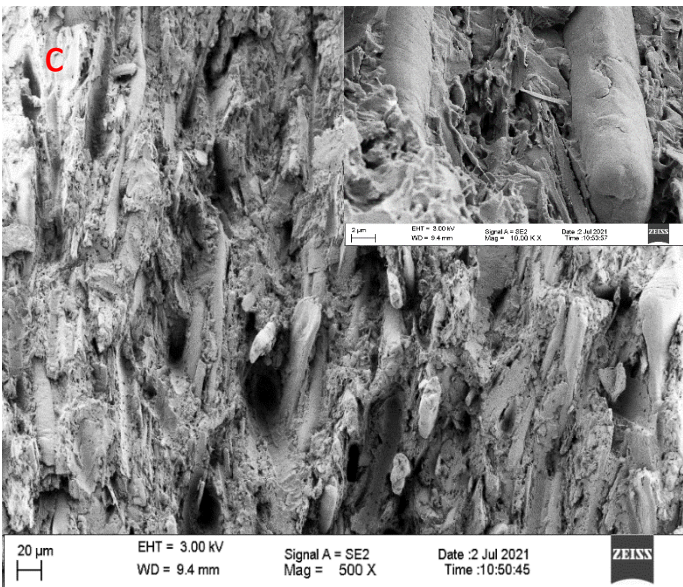
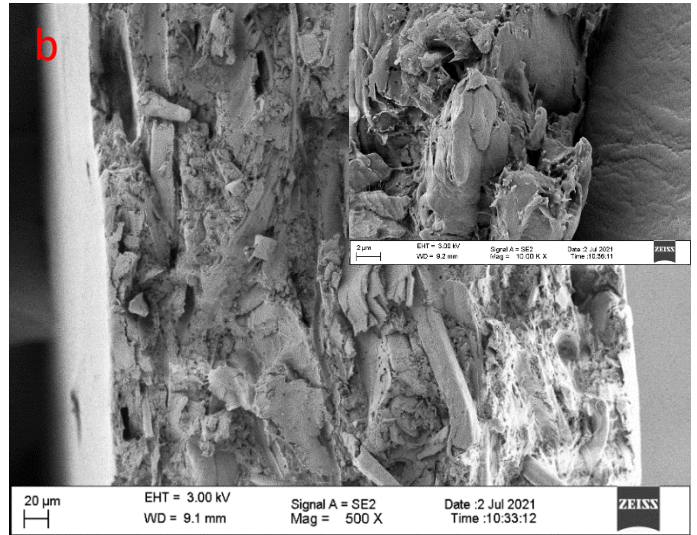
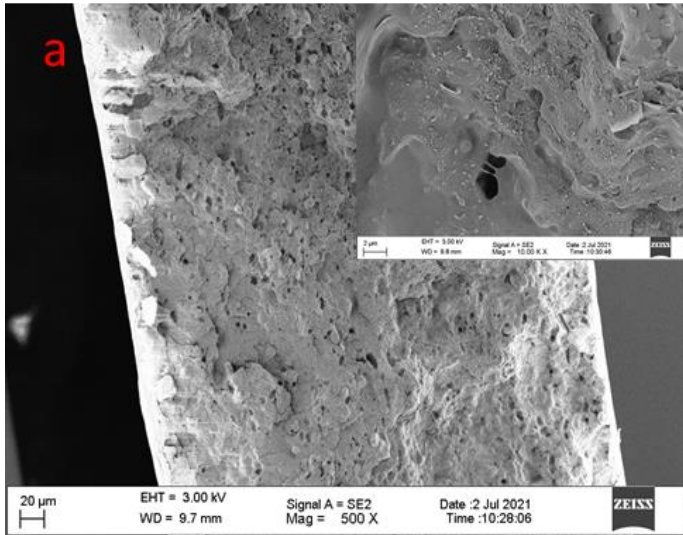


**Figure 7.** SEM images of the surface structure of TMP fibres after AKD modification using a) PP, b) PP-TMP, c) PP-TMP AKD Hex, d) PP-TMP AKD Lau and e) PP-TMP AKD St., Magnitudes: 500x & 10000x.

#### 4.4 The effects of MgSt, MoS<sub>2</sub> and AKD on the mechanical properties of TMP composites

The effects of MgSt and MoS<sub>2</sub> on the mechanical properties of the composites are reported in Table 6. Young's modulus, which has its highest increase at the highest loading content of 70 wt% of TMP, improved by a factor of 8.1 for the TMP-based samples compared to the matrix. The addition of lubricants at the same reinforcement content (i.e. 70 wt%) further improved the Young modulus by a factor of 10.7 for the TMP-based samples containing MoS<sub>2</sub>. In the samples without additives, the TMP-reinforced samples showed an improvement in the stress at break: from 24 MPa for EAA to 28 MPa at 30 wt%, and to 38 MPa at 50 wt% TMP (the bolded numbers in Table 6).

The elongation at break, a property that can be used to compare the ductility of these samples, was reduced drastically with the addition of TMP without any additives: from 491 % for the EAA to 4 % at 30 wt% TMP. For the 30 wt% TMP-composites, the addition of MgSt or MoS<sub>2</sub> improved the stress at break, the elongation at break and the impact strength (the bold numbers in Table 6). At 50 wt% TMP content, the addition of MgSt and MoS<sub>2</sub> decreased the stress at break: this can be due to the increase in ductility caused by the additives, which is expected.

At 70 wt% TMP content, despite the increase in Young's modulus from 2.4 GPa to 2.9 GPa and to 3.1 GPa for MgSt and MoS<sub>2</sub>, respectively, no significant changes were seen in the strength and elongation of the composites. In this case the reinforcement, i.e. the TMP, is more dominant than the matrix; at this high wt% content of TMP, neither of the additives could have a significant effect on the interface. It could, however, be due to the low amount of lubrication and it was therefore decided to increase the wt% of the lubricants in the TMP30 samples to see if that would improve matters.

The TMP30 samples with the lubricants added separately showed the largest improvement in mechanical properties, so it was at these concentrations of TMP that the effects of higher contents of lubricant were explored. When the amount of lubricant increased from 1.5 wt% to 5 wt% in the TMP30 composites, see Table 6, their mechanical properties exhibited clear changes, with the samples containing MgSt showing a decrease in both Young's modulus and strength. Despite the increase in the lubricant content, the MoS<sub>2</sub>-based TMP30 samples exhibited enhanced mechanical properties, which supports the argument of improved dispersion and interface between the TMP and the matrix due to the interaction between lignin and MoS<sub>2</sub><sup>58</sup>.

**Table 6.** Mechanical properties of the TMP-based composites with EAA as the matrix (standard deviation in parenthesis).

Sample	Young's modulus (GPa)	Stress at break (MPa)	Elongation at break (%)	Izod impact strength (kJ/m <sup>2</sup> )
EAA	<b>0.3 (0.06)</b>	<b>24 (1)</b>	<b>491 (20)</b>	-----
EAA-TMP30	<b>1.4 (0.1)</b>	<b>28 (2)</b>	<b>4 (1)</b>	<b>6 (1)</b>
EAA-TMP30-MgSt	1.5 (0.1)	35 (2)	5 (1)	7 (1)
EAA-TMP30-MoS <sub>2</sub>	<b>1.2 (0.1)</b>	<b>33 (1)</b>	<b>6 (1)</b>	<b>8 (1)</b>
EAA-TMP30-MgSt/MoS <sub>2</sub>	1.2 (0.1)	33 (3)	5 (3)	10 (1)
EAA-TMP30-5MgSt	1.4 (0.1)	32 (3)	4 (0.1)	7 (1)
EAA-TMP30-5MoS <sub>2</sub>	1.6 (0.1)	39 (1)	5 (0.1)	11 (2)
EAA-TMP30-2.5(MgSt+MoS <sub>2</sub> )	1.3 (0.1)	27 (3)	3 (0.4)	7 (2)
EAA-TMP50	<b>2.2 (0.03)</b>	<b>38 (1)</b>	<b>3 (1)</b>	
EAA-TMP50-MgSt	1.7 (0.08)	30 (5)	3 (1)	
EAA-TMP50-MoS <sub>2</sub>	<b>1.8 (0.3)</b>	<b>29 (3)</b>	<b>3 (1)</b>	
EAA-TMP50-MgSt/MoS <sub>2</sub>	1.6 (0.3)	27 (4)	3 (1)	
EAA-TMP70	2.4 (0.4)	33 (11)	3 (1)	
EAA-TMP70-MgSt	2.9 (0.4)	32 (6)	2 (1)	
EAA-TMP70-MoS <sub>2</sub>	3.1 (0.1)	31 (6)	3 (1)	

The effects of the AKDs on the mechanical properties of the composites are given in Table 7. The Young modulus of the composites can be seen to improve by a factor of 2 for the unmodified TMP-based samples compared to the PP matrix. Modifying TMP with AKD Hex and AKD Lau (the two shorter carbon chain lengths) generates materials with mechanical properties similar to unmodified TMP-PP composites (Table 7), whilst modifying with AKD St generates a composite with reduced strength when compared to the other materials tested.

This result is in agreement with a study by Quillin *et al.*<sup>15</sup> who showed that modifying bleached kraft cellulose pulp with long chain AKDs reduced the strength of the composites.

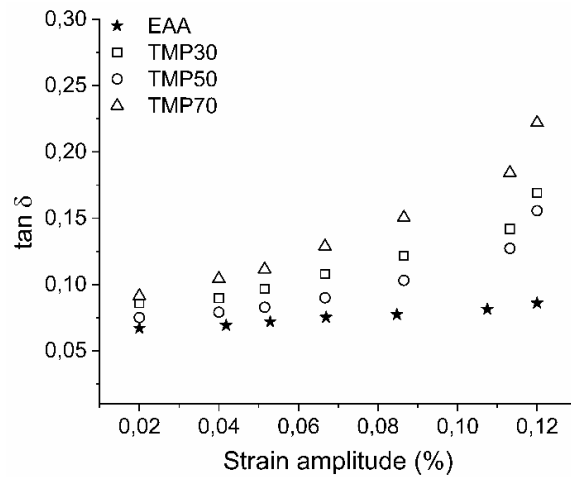
**Table 7.** Mechanical properties of the TMP modified with AKD with PP as the matrix (standard deviation in parenthesis).

Sample	Young's modulus (GPa)	Tensile stress at break (MPa)	Elongation at break (%)
PP	1.5	19	2.4
PP-TMP	3.1 (0.1)	11 (0.7)	0.4 (0.1)
PP-TMP AKD Hex	3 (0.3)	11 (2.3)	0.5 (0.1)
PP-TMP AKD Lau	3.4 (0.1)	9 (2.5)	0.4 (0.1)
PP-TMP AKD St	2.2 (0.3)	5 (0.9)	0.3 (0.1)

Overall, TMP-based composites have a higher strength than a pure matrix (EAA or PP). The addition of MgSt and MoS<sub>2</sub> to TMP-EAA composites increases the ductility of the samples, whereas the AKD modification of TMP shows no change in the ductility of the samples of TMP-PP composites.

#### 4.5 The effects of MgSt and MoS<sub>2</sub> on the interfacial properties of the composites

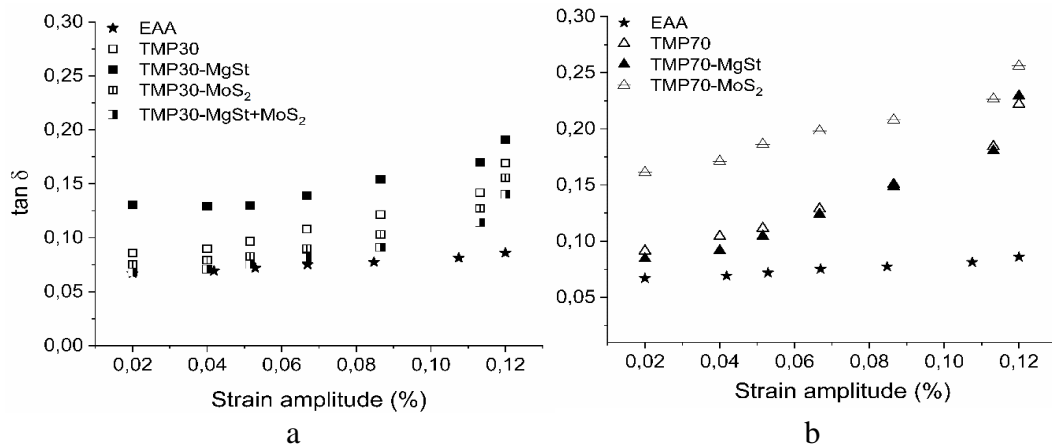
The ratio between the loss modulus ( $G''$ ) and the storage modulus ( $G'$ ), known as the damping factor or  $\tan \delta$ , provides information of the interface between the matrix and the pulp, with the relationship being: the larger the value of  $\tan \delta$ , the poorer quality of the interface<sup>66</sup>. The damping factor, i.e.  $\tan \delta$ , is shown as a function of the strain applied to EAA and EAA/TMP composites in Figure 8. The  $\tan \delta$  of the 70 wt% TMP composites is higher than the lower loads of TMP-based composites, which indicates a weakening of the interface between the fibres and the EAA matrix; moreover, it increases with increasing strain amplitude. The increase in the slope of the loss factor curve, relative to the matrix, probably suggests that the interface region is weak, e.g. due to a poor degree of adhesion between the phases which, in turn, would promote friction losses during the imposed sinusoidal deformation<sup>67,68</sup>.



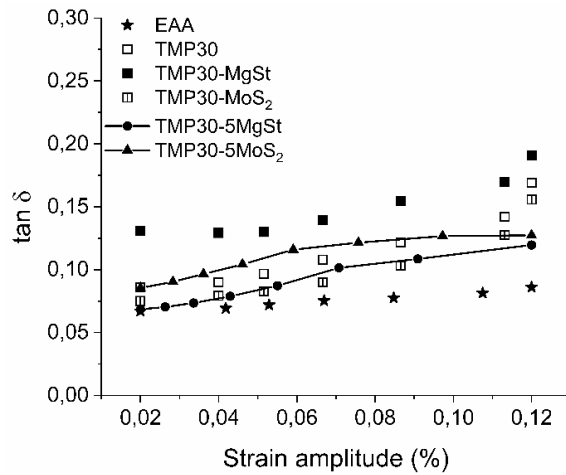
**Figure 8.** Mechanical loss factor as a function of the applied strain for composites with 30, 50 and 70 wt% TMP.

Figure 9 shows the effects the additives have on the interface of the 30 wt% TMP composites for the lowest and highest contents of TMP load. With the exception of the samples containing MgSt, those with lubricants and combinations thereof exhibited a  $\tan \delta$  dependence on the strain amplitude similar to that of the sample without any lubricant and close to the matrix, thereby suggesting a stronger interface region. This confirms the hypothesis that MoS<sub>2</sub> interacts more favourably than MgSt with TMP fibres. In Figure 9b (70 wt% TMP), all the samples exhibited  $\tan \delta$  relationships where the slopes remained similar to each other with increasing strain amplitude: they suggest a rather poor interface region, which could be expected as a result of the lower amount of EAA at this high level of loading.

When the lubricant concentration was increased from 1.5 wt% to 5 wt% in the TMP30 composite, the  $\tan \delta$  slope for the samples containing MgSt as the lubricant increased and the initial plateau observed at lower strain amplitudes, at a lubricant concentration of 1.5 wt%, was not observed (Figure 10). These results correlate to the mechanical properties given in Table 6, which showed a reduction in the overall mechanical performance as the concentration of lubricant increased in the composite. When the MoS<sub>2</sub> concentration was increased in the TMP composites, a plateau was observed at higher strain amplitudes that was not present for the TMP30 composite with 1.5 wt% MoS<sub>2</sub>: this is correlated with the increase in mechanical properties observed in Table 6.



**Figure 9.** Mechanical loss factor as a function of applied strain amplitudes for (a) 30 wt% and (b) 70 wt% TMP samples with MgSt and/or MoS<sub>2</sub>.



**Figure10.** Mechanical loss factor as a function of applied strain amplitude for 30 wt% TMP samples with varying amounts of MoS<sub>2</sub>. The lines are a guide for the eyes only

## 4.6 Melt shear viscosity and visual impression of modified and unmodified TMP-PP composites

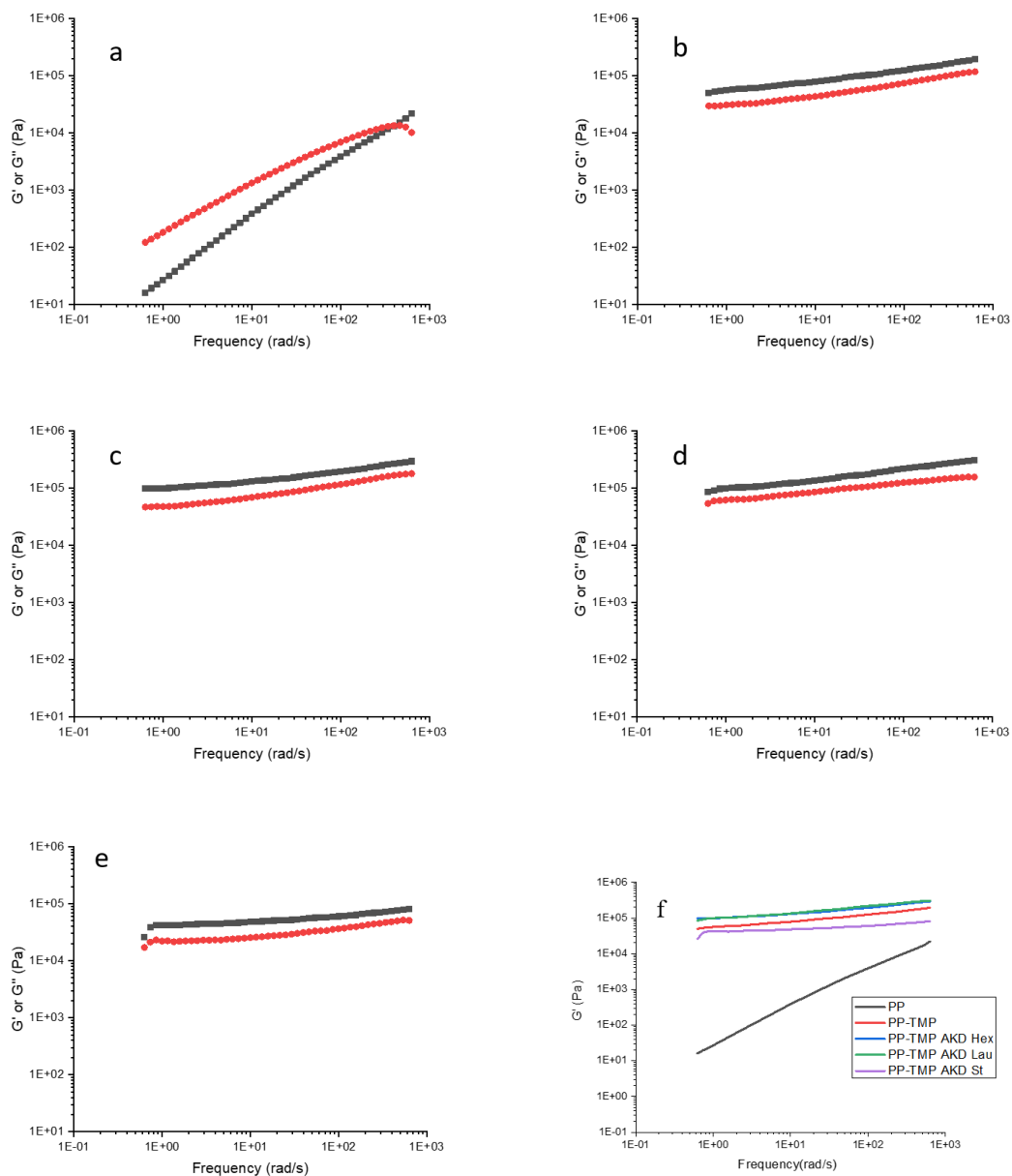


**Figure 11.** Frequency sweeps.  $G'$  (black) and  $G''$  (red) for (a) PP, (b) PP-TMP, (c) PP-TMP AKD Hex, (d) PP-TMP AKD Lau and (e) PP-TMP AKD St at 180 °C. (f)  $G'$  for different samples at 180 °C (N.B. the blue and green curves overlap).

The frequency dependence of the  $G'$  and  $G''$  of TMP-PP and AKD modified TMP-PP composites are shown in Figure 11, with the frequency sweep being recorded at 180°C. The addition of TMP to pure PP alters its frequency behaviour drastically. The PP matrix can be defined as a liquid (increasing moduli as a function of frequency, in combination with  $G'' > G'$ ) at the conditions measured, whereas TMP-PP composites tend to have larger absolute values



of moduli and  $G' > G''$ . This concurs with the rheology of fibre-PE composites as examined by Soucy *et al.*<sup>69</sup>. The rheological behaviour of the TMP-PP composite is not changed upon modification with AKDs having short carbon chains (AKD Hex and AKD Lau), although a small increase in absolute values of  $G'$  is observed. In contrast, a reduction in absolute values of  $G'$  is observed for the AKD St modified TMP -PP composites (see Figure 11f).

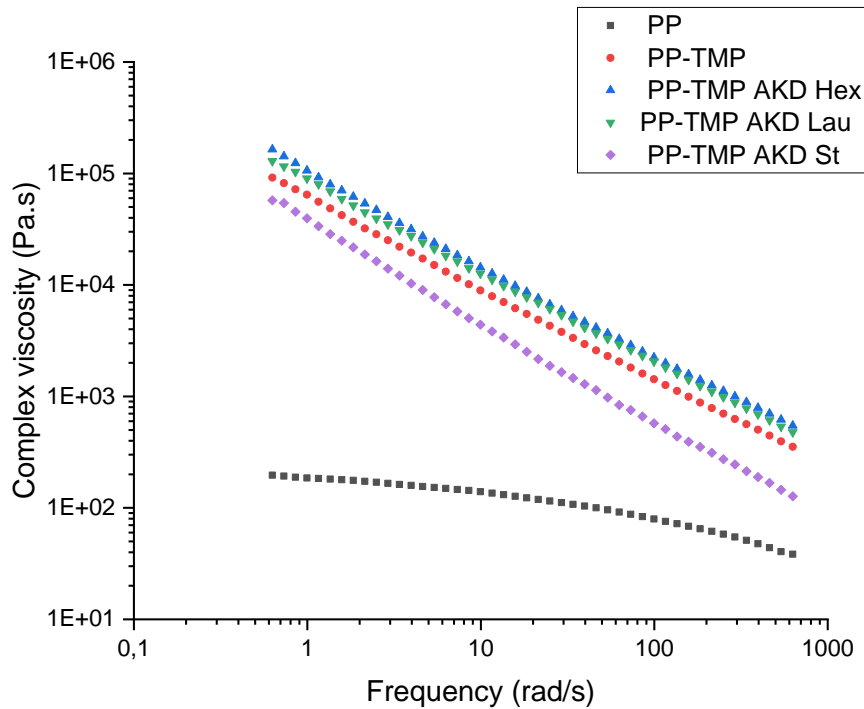


**Figure 12.** The complex viscosity obtained for pure PP, modified and unmodified TMP-based composites at 180 °C and a strain of 0.25%.

Figure 12 presents the variations in complex viscosity of neat PP, modified and unmodified TMP-based composites as a function of angular frequency. Although it can be observed that the complex viscosity decreases with increasing frequency for all samples, the slope of the curve is steeper for modified and unmodified TMP. The reduction in complex viscosity as a function of frequency can be seen as pseudoplastic characteristics, given that the Cox Merz rule would hold. However, the Cox-Merz rule is not applicable to highly filled systems: the hypothesis is put forward here that the increased slope of the complex viscosity is instead related to the reduction in space in the PP chains caused by the interlocked fibre network. The complex viscosity of PP-TMP AKD Hex and PP-TMP AKD Lau is higher than that of TMP-PP and PP; as shown in Figure 12, the complex viscosity of PP-TMP AKD St decreases compared to PP-

TMP, PP-TMP AKD Hex and PP-TMP AKD Lau. Although a small increase in both the moduli and viscosity upon modification of TMP with AKD Hex and Lau is observed, there is a decrease in the case of modification with AKD St. These results cannot be fully explained: indeed, studies have reported increasing as well as reducing moduli and viscosity upon the addition of additives. Reductions in viscosities and moduli has been explained as improved matrix fibre interaction, but these could also be related to fibre-fibre interactions being altered upon modification. Investigating the effects of AKD wax on the friction of paper-paper, Seppänen<sup>70</sup> showed that it caused a continuous reduction in friction between the pulp fibres. The decrease in the complex viscosity of the PP-TMP AKD St compared to the other samples can be due to the friction-reducing effect of fibre-fibre interactions in the composite system: AKD St therefore acts both as a compatibilizer and a lubricant in the system. This result is in agreement with Quillin *et al.* who showed that, with a mix of long chain AKDs, the AKD modification of bleached kraft pulp assisted the dispersibility of PP in composites with a high content of pulp<sup>15</sup>.

Figure 13 shows the extruded filaments of the modified and unmodified samples with a 50 wt% content of pure TMP fibres. Hatzikiriakos and Dealy<sup>71</sup> observed that, for neat PE, the surface of the extrudate filaments became gradually rougher as the pressure increased, and Hristov and Vlachopoulos<sup>72</sup> showed that the surface appearance of extrudate filaments of wood polymer composites is directly related to the shear rate and the pressure in the extruder. As can be seen in the figure, the AKD modification of TMP makes the extrudate filaments less rough, with the TMP AKD St having the smoothest surface of all the samples. The smoother surface of the AKD-modified TMP-PP filaments indicates that the processability of the modified samples, especially the TMP AKD St samples, increases; there is less wear and shear in the extrusion process, which is favourable for industrial applications.



**Figure 13.** Extruded filaments of a) PP-TMP, b) PP-TMP AKD Hex, c) PP-TMP AKD Lau and d) PP-TMP AKD St.

Another property that may be analyzed for extruded filaments is the die ratio ( $B_{swell}$ ), see Table 8, and decreases with chemical modification: here, AKD St has a  $B_{swell}=1$ . Ariffin *et al.*<sup>73</sup> have investigated the effect of shear stress on  $B_{swell}$  showing that, for filled and unfilled PP in general, the  $B_{swell}$  increases with increasing shear stress. The table shows that the TMP modified with AKD results in filaments with reduced values of  $B_{swell}$  and, in particular, that the TMP modified with AKD St shows no swelling at all. These results are indications of easier processing.

**Table 8.** Average diameter of extrudate filaments and die swell numbers.

An average of 10 measurements were made; the diameter was measured outside the pullout areas on the filament. Standard deviation is given in parenthesis.

Sample	Diameter (mm)	$B_{swell}$
PP-TMP	2.14 (0.07)	1.08
PP-TMP AKD Hex	2.02 (0.03)	1.02
PP-TMP AKD Lau	2.00 (0.03)	1.01
PP-TMP AKD St	1.99 (0.03)	1.00

The visual appearance of the dog bones made from PP, TMP-PP and modified TMP-PP composites are shown in Figure 14. It can be seen that the TMP AKD Lau and St samples have a brighter colour than the unmodified TMP sample, which is another indication of the enhanced ease of processing the composites with high contents of TMP. Local thermal degradation resulting from high shear stress is often used to explain the dark appearance of wood based composites<sup>74-76</sup>.

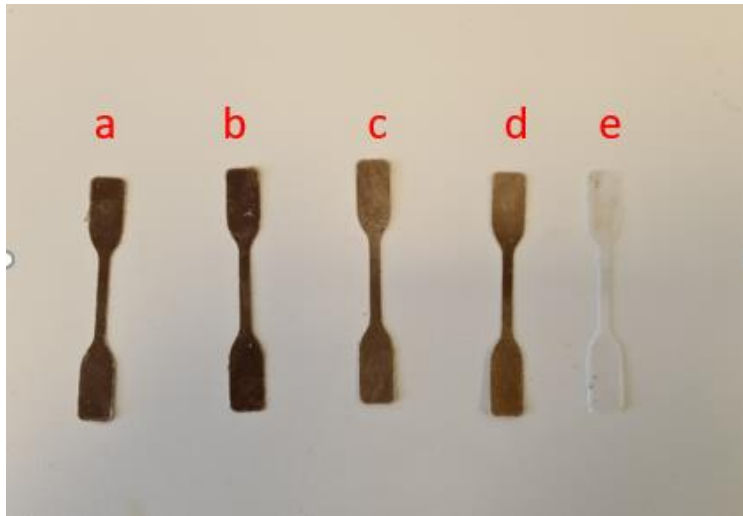


**Figure 14.** Dog bone samples of a) PP-TMP, b) PP-TMP AKD Hex, c) PP-TMP AKD Lau, d) PP-TMP AKD St and e) PP.

## 5 Conclusions

It has been shown that wet adsorption of MgSt and MoS<sub>2</sub> on pulp fibres is an efficient way of coating them with lubricant additives. Moreover, both MgSt and MoS<sub>2</sub> had a positive impact on the mechanical properties of the composites. The largest increase in the tensile modulus of the composites, a factor of 10.7, was noted for the TMP70-MoS<sub>2</sub> sample. The tensile properties and DMA studies showed that MoS<sub>2</sub> bonded better than MgSt with the TMP fibres.

The adsorption of MgSt and MoS<sub>2</sub> on TMP fibres was confirmed through EDX analysis. The observation that MoS<sub>2</sub> improved the interface region in TMP-matrix composites may be of importance when studying flow properties in the extrusion process of TMP-based composites. The chemical modification of TMP fibres with AKD was shown to have a significant effect on the surface energy and the contact angle: increasing the length of the carbon chain of the AKD made the surface of the modified fibres increasingly hydrophobic. The TMP modified with AKD St had the greatest water contact angle and the lowest surface energy, which are direct indications of hydrophobicity. AKD modification did not show an effect on the mechanical properties when compared to the unmodified TMP fibres, with the exception that AKD St reduced the tensile strength. The rheological studies showed that the TMP addition caused an increase in the complex viscosity of the PP. TMP modified with AKD Hex or AKD Lau caused a small increase in the complex viscosity, whilst TMP modified with AKD St decreased the complex viscosity of the composite compared to the TMP-PP melt. Visual impressions, such as the colour of the dog bones and the smoothness of the extrudate filaments, along with the die swell ratio, indicate that TMP modified with AKD St in particular facilitates the processing of TMP-PP composites.

## 6 Future work

An important aspect that requires further study is the interfacial properties of modified TMP fibres and the matrix in TMP composites:  $\tan \delta$  can provide information of the interface of the matrix and the pulp. While oscillatory shear rheology was carried out with the aim of studying the rheological properties of the composites, elongational rheology may be closer to the extrusion process and thus allow more information of the processing conditions to be revealed. This is of particular importance since it can lead to the processing of composites with a TMP fibre content that exceeds 50 wt%.

## 7 Acknowledgments

The generous funding of this work by The Swedish Foundation for Strategic Research, VINNOVA and Stora Enso is acknowledged.

I would like to express gratitude to the people who supported me during this study. First and foremost, thanks go to my supervisors Anna Ström, Anette Larsson and Gunnar Westman not only for their support and guidance but also for broadening the horizons of my ideas throughout my studies duration. I would like to give special thanks to my examiner, Lars Öhrström, the previous director of studies, Lars Evenäs, the current director of studies, Itai Panas and Nina Kann the former head of PhD students for their help and wisdom.

Sincere thanks are due to everyone in the Larsson-Ström-Nypelö group for their encouragement and support in both scientific and social aspects.

Last, but not least, I am very grateful to all the people in the Chemistry and Chemical Engineering and Industrial and Materials Science Departments at Chalmers University of Technology for their assistance, and especially so to the co-author of my first article, Abhijit Venkatesh, for helping me with the various different techniques and instruments.

Thank you!

## 8 Bibliography

1. Brooks, A. L., Wang, S. & Jambeck, J. R. The Chinese import ban and its impact on global plastic waste trade. *Sci Adv* **4**, (2018).
2. Circular Economy: new rules on single-use plastics. *European Commission - European Commission* [https://ec.europa.eu/commission/presscorner/detail/en/IP\\_19\\_2631](https://ec.europa.eu/commission/presscorner/detail/en/IP_19_2631).
3. The forest and sustainable forestry. *Swedish Wood* <https://www.swedishwood.com/wood-facts/about-wood/wood-and-sustainability/the-forest-and-sustainable-forestry/>.
4. Schirp, A. & Stender, J. Properties of extruded wood-plastic composites based on refiner wood fibres (TMP fibres) and hemp fibres. *European Journal of Wood Prod.* **68**, 219–231 (2010).
5. Yam, K. L., Gogoi, B. K., Lai, C. C. & Selke, S. E. Composites from compounding wood fibers with recycled high density polyethylene. *Polymer Engineering & Science* **30**, 693–699 (1990).
6. Mertens, O., Gurr, J. & Krause, A. The utilization of thermomechanical pulp fibers in WPC: A review: *Journal of Applied Polymer Science* **134**, 45161 (2017).
7. Nygård, P., Tanem, B. S., Karlsen, T., Brachet, P. & Leinsvang, B. Extrusion-based wood fibre–PP composites: Wood powder and pelletized wood fibres – a comparative study. *Composites Science and Technology* **68**, 3418–3424 (2008).
8. Lu, J. Z., Wu, Q. & Negulescu, I. I. Wood-fiber/high-density-polyethylene composites: Compounding process. *Journal of Applied Polymer Science* **93**, 2570–2578 (2004).
9. Schirp, A., Mannheim, M. & Plinke, B. Influence of refiner fibre quality and fibre modification treatments on properties of injection-moulded beech wood–plastic composites. *Composites Part A: Applied Science and Manufacturing* **61**, 245–257 (2014).
10. Liou, W. J. Stress distributions of short fiber composite materials. *Computers & Structures* **62**, 999–1012 (1997).
11. Experimental, analytical, and finite element study of stress concentration factors for composite materials - Makki, M.M. & Chokri, B. (2017). <https://journals.sagepub.com/doi/full/10.1177/0021998316659915>.

12. Maldas, D. & Kokta, B. V. Influence of phthalic anhydride as a coupling agent on the mechanical behavior of wood fiber–polystyrene composites. *Journal of Applied Polymer Science* **41**, 185–194 (1990).
13. Myers, G. E. *et al.* Extruded Wood-Flour Polypropylene Composites: Effect of a Maleated Polypropylene Coupling Agent on Filler-Matrix Bonding and Properties. *MRS Online Proceedings Library* **197**, 67–76 (1990).
14. Takase, S. & Shiraishi, N. Studies on composites from wood and polypropylenes. II. *Journal of Applied Polymer Science* **37**, 645–659 (1989).
15. Quillin, D. T., Caulfield, D. F. & Koutsky, J. A. Cellulose/Polypropylene Composites: The Use of AKD and ASA Sizes as Compatibilizers. *International Journal of Polymeric Materials and Polymeric Biomaterials* **17**, 215–227 (1992).
16. Liu, W. *et al.* Lignin-assisted exfoliation of molybdenum disulfide in aqueous media and its application in lithium ion batteries. *Nanoscale* **7**, 9919–9926 (1394).
17. Donnet, C. & Erdemir, A. Historical developments and new trends in tribological and solid lubricant coatings. *Surface and Coatings Technology* **180–181**, 76–84 (2004).
18. Ghaffar, S. H., Madyan, O. A., Fan, M. & Corker, J. The Influence of Additives on the Interfacial Bonding Mechanisms Between Natural Fibre and Biopolymer Composites. *Macromol. Res.* **26**, 851–863 (2018).
19. Sizing of Paper, Third Edition. <https://imisrise.tappi.org/TAPPI/Products/01/R/0101R311.aspx>.
20. Konaka, Y., Sawada, K., 小中美紀 & 澤田公平. Magnesium stearate for elastic fiber and method for producing the same. (2004).
21. Varnell, D. F. Process for surface sizing paper and paper prepared thereby. (2000).
22. Lindström, T. & Larsson, P. T. Alkyl ketene dimer (AKD) sizing : A review. *Nordic Pulp & Paper Research Journal* **23**, 202–209 (2008).
23. Saarikoski, E., Lipponen, S., Rissanen, M. & Seppälä, J. Blending cellulose with polyethylene-co-acrylic acid in alkaline water suspension. *Cellulose* **19**, 661–669 (2012).



24. Recchia, F. P., Ferrell, W. M. & Jr, W. M. F. High solids ethylene acrylic acid aqueous dispersions and methods of producing same. (1997).
25. Park, J. *et al.* Use of mechanical refining to improve the production of low-cost sugars from lignocellulosic biomass. *Bioresource Technology* **199**, 59–67 (2016).
26. Hasani, M. Chemical modification of cellulose-new possibilities of some classical routes. (Chalmers University of Technology, 2010).
27. Heinemann, S., Kleen, M., Wang, S. & Peltonen, J. Mechanical Pulping: Characterization of fiber wall surface structure of chemically modified TMP fibers from Norway spruce. *Nordic Pulp & Paper Research Journal* **26**, 21–30 (2011).
28. Kangas, H. & Kleen, M. Surface chemical and morphological properties of mechanical pulp fines. *Nordic Pulp & Paper Research Journal* **19**, 191–199 (2004).
29. CELLULOSE ALLOMORPHS – OVERVIEW AND PERSPECTIVES.  
[http://www.novapublishers.org/catalog/product\\_info.php?products\\_id=14044](http://www.novapublishers.org/catalog/product_info.php?products_id=14044).
30. Bledzki, A. K. & Gassan, J. Composites reinforced with cellulose based fibres. *Progress in Polymer Science* **24**, 221–274 (1999).
31. Wang, S., Sun, Y., Kong, F., Yang, G. & Fatehi, P. Preparation and Characterization of Lignin-Acrylamide Copolymer as a Paper Strength Additive. *BioResources* **11**, 1765–1783 (2016).
32. Bajpai, P. Chapter 2 - Wood and Fiber Fundamentals. in *Biermann's Handbook of Pulp and Paper (Third Edition)* (ed. Bajpai, P.) 19–74 (Elsevier, 2018). doi:10.1016/B978-0-12-814240-0.00002-1.
33. Olakanmi, E. O. & Strydom, M. J. Critical materials and processing challenges affecting the interface and functional performance of wood polymer composites (WPCs). *Materials Chemistry and Physics* **171**, 290–302 (2016).
34. Peltola, H., Pääkkönen, E., Jetsu, P. & Heinemann, S. Wood based PLA and PP composites: Effect of fibre type and matrix polymer on fibre morphology, dispersion and composite properties. *Composites Part A: Applied Science and Manufacturing* **61**, 13–22 (2014).

35. Liu, K., Zhang, C. & Madbouly, S. A. 10 - Fiber Reinforced Plant Oil-Based Composites. in *Bio-Based Plant Oil Polymers and Composites* (eds. Madbouly, S. A., Zhang, C. & Kessler, M. R.) 167–189 (William Andrew Publishing, 2016). doi:10.1016/B978-0-323-35833-0.00010-4.
36. Duc, F., Bourban, P. E., Plummer, C. J. G. & Månson, J.-A. E. Damping of thermoset and thermoplastic flax fibre composites. *Composites Part A: Applied Science and Manufacturing* **64**, 115–123 (2014).
37. Ariño, R. & Boldizar, A. Processing and mechanical properties of thermoplastic composites based on cellulose fibers and ethylene—acrylic acid copolymer. *Polymer Engineering & Science* **52**, 1951–1957 (2012).
38. Wu, J., Yu, D., Chan, C.-M., Kim, J. & Mai, Y.-W. Effect of fiber pretreatment condition on the interfacial strength and mechanical properties of wood fiber/PP composites. *Journal of Applied Polymer Science* **76**, 1000–1010 (2000).
39. Joseph, P. M. Effect of processing variables on the mechanical properties of sisal-fiber-reinforced polypropylene composites. *Composites science and technology* (1999) doi:10.1016/S0266-3538(99)00024-X.
40. Oksman, K. & Lindberg, H. Interaction Between Wood and Synthetic Polymers. **49**, 249–254 (1995).
41. Maldas, D. & Kokta, B. V. Influence of maleic anhydride as a coupling agent on the performance of wood fiber-polystyrene composites. *Polymer Engineering & Science* **31**, 1351–1357 (1991).
42. Bae, C.-J., Kim, H.-W., Koh, Y.-H. & Kim, H.-E. Hydroxyapatite (HA) bone scaffolds with controlled macrochannel pores. *Journal of Material Science: Materials in Medicine* **17**, 517–521 (2006).
43. Bruce, R. W. *Handbook of Lubrication and Tribology, Volume II : Theory and Design, Second Edition*. (CRC Press, 2012). doi:10.1201/b12265.
44. Lee, S., Shupe, T. F. & Hse, C. Y. Thermosets as compatibilizers at the isotactic polypropylene film and thermomechanical pulp fiber interphase. *Composite Interfaces* **15**, 221–230 (2008).

45. Yadgarov, L. *et al.* Tribological studies of rhenium doped fullerene-like MoS<sub>2</sub> nanoparticles in boundary, mixed and elasto-hydrodynamic lubrication conditions. *Wear* **297**, 1103–1110 (2013).
46. Uzunovic, A. & Vranic, E. Effect of magnesium stearate concentration on dissolution properties of ranitidine hydrochloride coated tablets. *Bosnian J. Basic Med. Sci.* **7**, 279–283 (2007).
47. Odeniyi, M. A., Alfa, J. & Jaiyeoba, K. T. Effect of Lubricants on Flow Properties and Tablet Strength of Silicified Microcrystalline Cellulose. **6** (2008).
48. Dankovich, T. A. & Hsieh, Y.-L. Surface modification of cellulose with plant triglycerides for hydrophobicity. *Cellulose* **14**, 469–480 (2007).
49. Rozman, H. D., Khalil, H. P. S. A., Kumar, R. N., Abusamah, A. & Kon, B. K. Improvements of Fibreboard Properties through Fibre Activation with Silane. *International Journal of Polymeric Materials and Polymeric Biomaterials* **32**, 247–257 (1996).
50. Kazayawoko, M., Balatinecz, J. J. & Matuana, L. M. Surface modification and adhesion mechanisms in woodfiber-polypropylene composites. *Journal of Materials Science* **34**, 6189–6199 (1999).
51. Kazayawoko, M., Balatinecz, J. J. & Woodhams, R. T. Diffuse reflectance Fourier transform infrared spectra of wood fibers treated with maleated polypropylenes. *Journal of Applied Polymer Science* **66**, 1163–1173 (1997).
52. Schirp, A. & Schirp, C. Online Pre-Treatment of Thermomechanical Pulp with Emulsified Maleated Polypropylene for Processing of Extruded Thermoplastic Composites. *Fibers* **9**, 17 (2021).
53. Lee, S., Shupe, T. F., Groom, L. H. & Hse, C. Y. Thermomechanical pulp fiber surface modification for enhancing the interfacial adhesion with polypropylene. *Wood and Fiber Science, Vol. 39(3)*: 424-433 (2007).
54. Xie, H. *et al.* Highly compatible wood thermoplastic composites from lignocellulosic material modified in ionic liquids: Preparation and thermal properties. *Journal of Applied Polymer Science* **111**, 2468–2476 (2009).

55. George, M., Mussone, P. G. & Bressler, D. C. Surface and Bulk Transformation of Thermomechanical Pulp Using Fatty Acyl Chlorides: Influence of Reaction Parameters on Surface, Morphological, and Thermal Properties. *Journal of Wood Chemistry and Technology* **36**, 114–128 (2016).
56. Teacă, C. & Tanasă, F. Wood Surface Modification—Classic and Modern Approaches in Wood Chemical Treatment by Esterification Reactions. (2020) doi:10.3390/coatings10070629.
57. Kumar, S., Chauhan, V. S. & Chakrabarti, S. K. Separation and analysis techniques for bound and unbound alkyl ketene dimer (AKD) in paper: A review. *Arabian Journal of Chemistry* **9**, S1636–S1642 (2016).
58. Hosseini, S., Venkatesh, A., Boldizar, A. & Westman, G. Molybdenum disulphide—A traditional external lubricant that shows interesting interphase properties in pulp-based composites. *Polymer Composites*. 16 (2021).
59. Isabel Moutinho, Margarida Figueiredo, and Paulo Ferreira. Evaluating the Surface Energy of Laboratory-Made Paper Sheets by Contact Angle Measurements, TAPPI J. <https://imrise.tappi.org/TAPPI/Products/07/JUN/07JUN26.aspx>.
60. Seo, W.-S., Cho, N.-S. & Ohga, S. Possibility of Hydrogen Bonding between AKD and Cellulose Molecules during AKD Sizing. *J. Fac. Agric. Kyushu Univ.* **53**, 405–410 (2008).
61. Carvalho, M. G., Santos, J. M. R. C. A., Martins, A. A. & Figueiredo, M. M. The Effects of Beating, Web Forming and Sizing on the Surface Energy of Eucalyptus globulus Kraft Fibres Evaluated by Inverse Gas Chromatography. *Cellulose* **12**, 371–383 (2005).
62. Huang, Y., Gardner, D. J., Chen, M. & Biermann, C. J. Surface energetics and acid-base character of sized and unsized paper handsheets. *Journal of Adhesion Science and Technology* **9**, 1403–1411 (1995).
63. Graziano, A., Jaffer, S. & Sain, M. Review on modification strategies of polyethylene/polypropylene immiscible thermoplastic polymer blends for enhancing their mechanical behavior. *Journal of Elastomers & Plastics* **51**, 291–336 (2019).

64. Arminger, B., Gindl-Altmutter, W., Keckes, J. & Hansmann, C. Facile preparation of superhydrophobic wood surfaces via spraying of aqueous alkyl ketene dimer dispersions. *RSC Adv.* **9**, 24357–24367 (2019).
65. Onda, T., Shibuichi, S., Satoh, N. & Tsujii, K. Super-Water-Repellent Fractal Surfaces. *Langmuir* **12**, 2125–2127 (1996).
66. Kubát, J., Rigdahl, M. & Seldén, R. Internal stresses and activation volumes from the stress relaxation behavior of polyethylene at low deformations. *Journal of Applied Polymer Science* **20**, 2799–2809 (1976).
67. Forsgren, L. *et al.* Composites with surface-grafted cellulose nanocrystals (CNC). *Journal of Materials Science* **54**, 3009–3022 (2019).
68. Kubát, J., Rigdahl, M. & Welander, M. Characterization of interfacial interactions in high density polyethylene filled with glass spheres using dynamic-mechanical analysis. *Journal of Applied Polymer Science* **39**, 1527–1539 (1990).
69. Soucy, J., Godard, F., Rivard, P. & Koubaa, A. Rheological behavior of high-density polyethylene (HDPE) filled with paper mill sludge. *Journal of Applied Polymer Science* **135**, 46484 (2018).
70. Seppänen, R. On the Internal Sizing Mechanisms of Paper with AKD and ASA Related to Surface Chemistry, Wettability and Friction. (2007).
71. Chen, Y.-L., Larson, R. G. & Patel, S. S. Shear fracture of polystyrene melts and solutions. *Rheologica Acta* **33**, 243–256 (1994).
72. Hristov, V. & Vlachopoulos, J. Effects of polymer molecular weight and filler particle size on flow behavior of wood polymer composites. *Polymer Composites* **29**, 831–839 (2008).
73. Ariffin, A., Ariff, Z. M. & Jikan, S. S. Evaluation on extrudate swell and melt fracture of polypropylene/kaolin composites at high shear stress. *Journal of Reinforced Plastics and Composites* **30**, 609–619 (2011).
74. TREJO-O'REILLY, J.-A., CAVAILLE, J.-Y. & GANDINI, A. The surface chemical modification of cellulosic fibres in view of their use in composite materials. *Cellulose* **4**, 305–320 (1997).

75. George, J., Sreekala, M. S. & Thomas, S. A review on interface modification and characterization of natural fiber reinforced plastic composites. *Polymer Engineering & Science* **41**, 1471–1485 (2001).
76. Baiardo, M., Frisoni, G., Scandola, M. & Licciardello, A. Surface chemical modification of natural cellulose fibers. *Journal of Applied Polymer Science* **83**, 38–45 (2002).

## 9 Appendix

### 9.1 NMR spectra of synthesized AKD

Three different AKD molecules were synthesized, namely AKD Hex, AKD Lau and AKD St. The  $^1\text{H}$  NMR signals obtained for the AKD Hex were as follows:  $^1\text{H}$  NMR (399.95 MHz,  $\text{CDCl}_3$ )  $\delta$ : 4.71 (t, 1H), 3.97 (t, 1H), 2.17 (m, 2H), 1.78 (m, 4H), 1.2-1.75 (m, mixture of alkyl chains) and 0.92 (m, 3H). Trace amounts of impurities (mostly the unfiltered produced salt and butyl acetate (the solvent) were present.

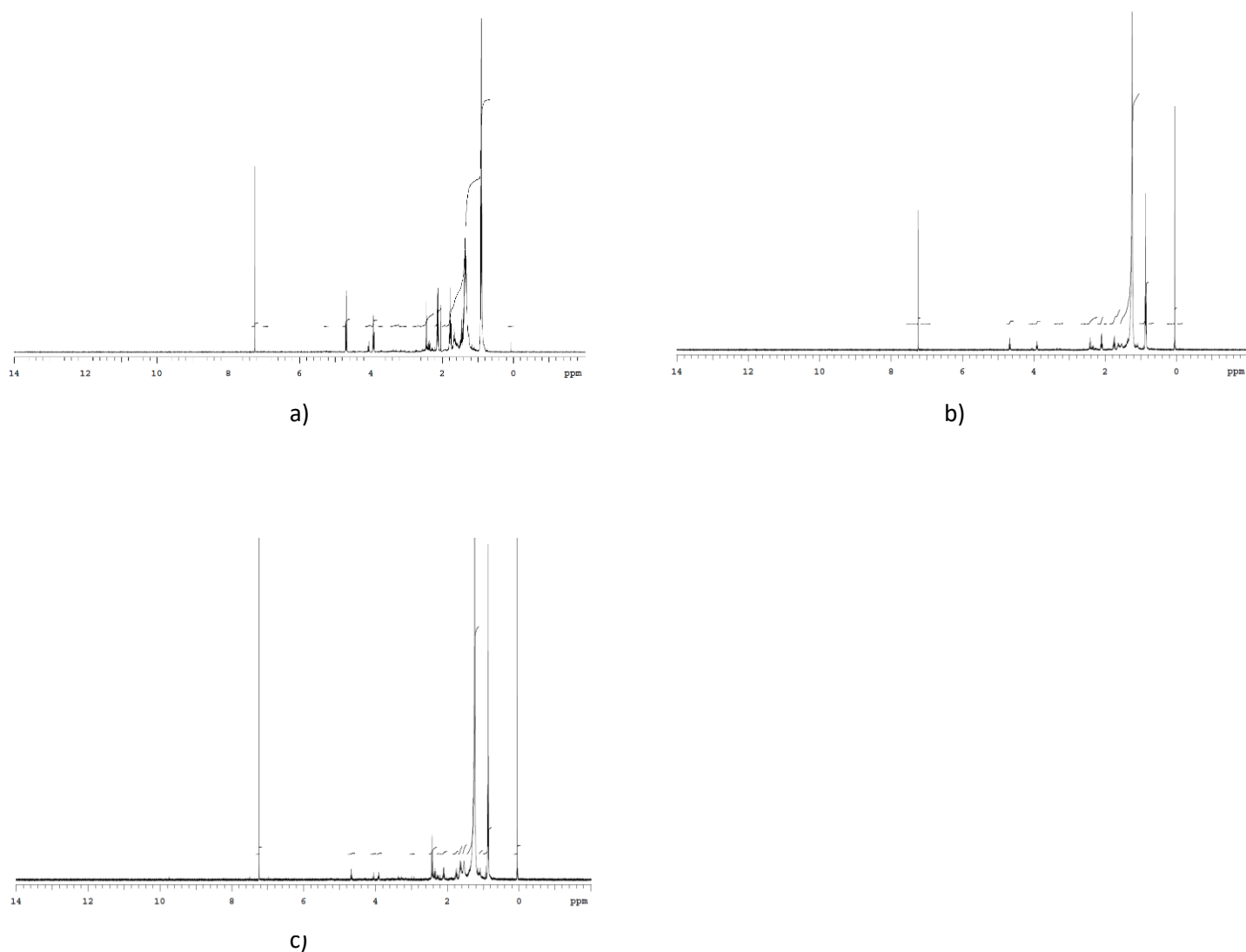


**Figure S1.**  $^1\text{H}$  NMR spectra obtained for AKD from a) hexanoyl chloride, b) lauryl chloride and c) stearoyl chloride (200 MHz,  $\text{CDCl}_3$  solution).

## 9.2 Water drop volume and water contact angle over time

In each modification, the water drop volume and water contact angle stabilized after some moments. As expected, the longer the carbon chain on the AKD molecule, the more voluminous the drop on the surface, and the larger the water contact angle after stabilization of the drop on the surface (see Figures S2 and S3).

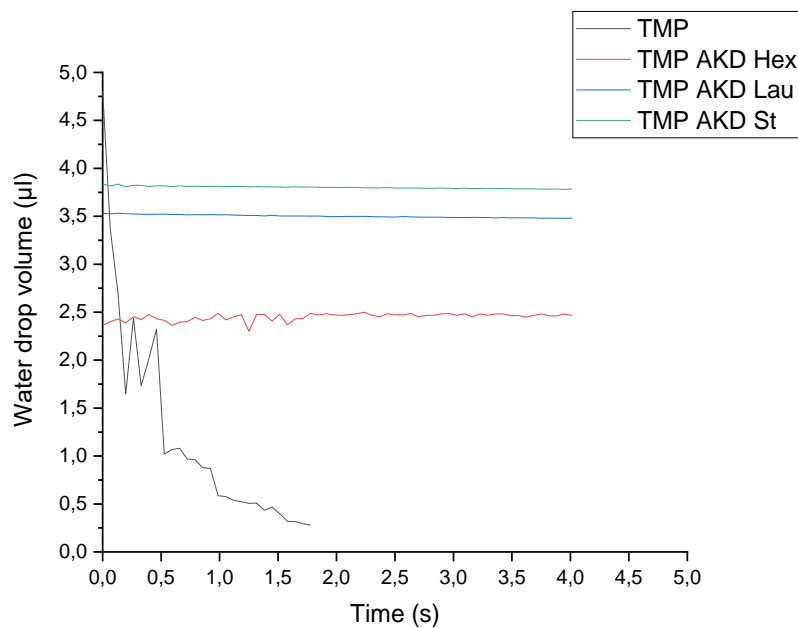


**Figure S2.** Surface wettability determined by measuring the progression of the water drop volume over time for unmodified fibres of TMP (black), TMP AKD Hex (red), TMP AKD Lau (blue) and TMP AKD St (green).



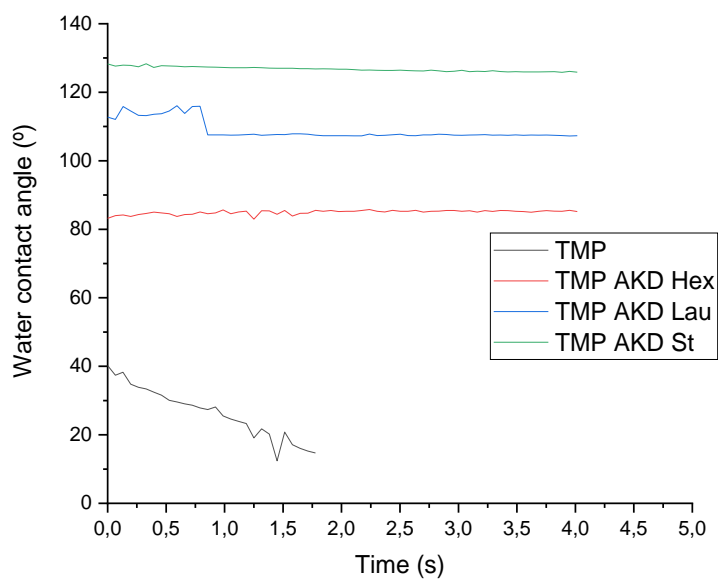


**Figure S3.** Progression of the water contact angle over time for unmodified fibres of TMP (black), TMP AKD Hex (red), TMP AKD Lau (blue) and TMP AKD St (green).

### 9.3 Thermal degradation of the modified TMP fibres

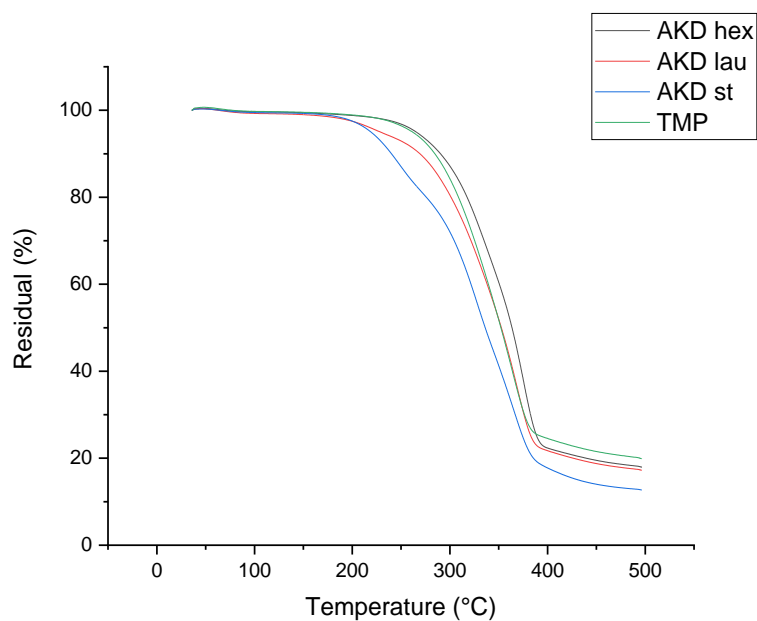


**Figure S4.** Thermogravimetric curves of the thermal degradation of modified TMP fibres.